Electric Vehicles Mass Integration: Impact on the Power Grid and Charging Infrastructure Availability

Joseph Antoun

A Thesis

in

The Department

of

Electrical and Computer Engineering

Presented in Partial Fulfillment of the Requirements for the Degree of

Master of Applied Science (Electrical and Computer Engineering) at

Concordia University

Montréal, Québec, Canada

November 2020

CONCORDIA UNIVERSITY

School of Graduate Studies

This is to certify that the thesis prepared

By: Joseph Antoun

Entitled: **Electric Vehicles Mass Integration: Impact on the Power Grid and Charging Infrastructure Availability**

and submitted in partial fulfillment of the requirements for the degree of

Master of Applied Science (Electrical and Computer Engineering)

complies with the regulations of this University and meets the accepted standards with respect to originality and quality.

Signed by the Final Examining Committee:

_____ Chair
Dr. M.K. Mehmet Ali

_____ External Examiner
Dr. Walter Lucia (CIISE)

_____ Examiner
Dr. M.K. Mehmet Ali

_____ Supervisor
Dr. Chadi Assi (CIISE)

_____ Co-supervisor
Dr. Ribal Atallah (Hydro-Quebec)

Approved by _____
Dr. Y.R. Shayan, Chair
Department of Electrical and Computer Engineering

_____ 2020

_____
Dr. Mourad Debbabi, Interim Dean,
Gina Cody School of Engineering and Computer Science

Abstract

Electric Vehicles Mass Integration: Impact on the Power Grid and Charging Infrastructure Availability

Joseph Antoun

Electric Vehicles (EV) are gaining large popularity in the transportation sector, and that raises numerous concerns for the power sector. The repercussions of such increased demand are notable at the distribution side with different aspects of EV usage. To accommodate this increased number, multiple Charging Stations (CS) are being deployed to assist users in enhancing their charging experience. However, public stations are underutilized due to lack of useful performance information, such as waiting time, and outlet availability. Therefore, users will favor home charging over public charging. This behavior will come with a drastic increase in power demand on the residential network. In addition, various behaviors of EV users, such as mass charging and preconditioning, can deteriorate the network's Quality-of-Service (QoS). Therefore, the impact of an elevated number of EVs and increased number of level 2 chargers on the residential distribution network is analyzed. Subsequently, the competency of dynamic pricing in handling this such elevated load in investigated. Afterwards, the repercussions from users preconditioning their vehicles during winter is inspected. In addition, we assess the competency of network reconfiguration in holding the network performance within operational range during preconditioning window. The performance of network reconfiguration will degrade when presented with high number of EVs; therefore this elevated number is leveraged through Vehicle-to-Grid (V2G) technology to assist network reconfiguration in balancing the preconditioning load. Finally, a data-driven performance model for public charging stations is derived to gain more knowledge on its operation. Metrics such as waiting time, reneging probability and blocking probability are derived and analyzed to assist users in their charging processes and operators enhancing the station deployment.

Acknowledgments

I would like to express my deepest gratitude to my supervisor, Dr. Chadi Assi, who has always been an inspiration for his knowledge and work ethics. The two years working with him to complete this thesis has been educational and fulfilling.

I would also like to express my appreciation to my co-supervisor, Dr. Ribal Atalah, for his constant support and mentorship.

I would also like to thank Dr. Maurice Khabbaz, Dr. Bassam Moussa, and Dr. Mohsen Ghafoury, the wonderful research mentor that I had the chance to work with during the making of this thesis.

In addition, I have been incredibly lucky to have the most amazing colleagues in the Lab. Their encouragement and advice have been indispensable at times of hardship and frustration.

Most importantly, I would like to thank my parents and my friends, who have always believed in me and supported me throughout this thesis.

Contents

List of Figures

List of Tables

List of Symbols

0.1 Impact Analysis of Level 2 EV Chargers on Residential Power Distribution Grids

- λ: Electric Vehicles charging requests' arriving rate
- T: Charging time
- β: Battery Capacity
- SoC: Battery State of Charge
- ζ: Charging power rate
- V_{n+1}: Voltage Magnitude at node n+1
- V_n: Voltage Magnitude at node n
- P_n: Active power flow from node n to n+1
- Q_n: Reactive power flow from node n to n+1
- r_n: Line resistance between node n and n+1
- x_n: Line reactance between node n and n+1
- t: Pricing threshold
- α: Electric Vehicles adoption rate
- σ: Level 2 charger penetration rate
- R: Number of residences

0.2 Assisting Residential Distribution Grids in Overcoming Large Scale EV Preconditioning Load

- λ: Electric vehicles charging request arrival rate
- τ: Charging time
- SoC: Battery State of Charge
- Φ: Battery Capacity
- ζ: Charging rate
- π: Electric vehicles preconditioning request arrival rate
- α: Electric vehicle adoption rate
- σ: Level 2 chargers penetration rate
- P_{loss}: Active system power loss
- Q_{loss}: Reactive system power loss
- N_{EV}: Number of electric vehicles
- N_L: Number of load elements
- N_C: Number of capacitor banks
- P_{feeder}: Active power entering the system
- Q_{feeder}: Reactive power entering the system
- P_{load}: Active power from load elements
- Q_{load}: Reactive power from load elements
- P_{EV}: Active load from electric vehicles
- Q_{EV}: Reactive load from electric vehicles
- P_C: Active load from capacitor banks
- Q_C: Reactive load from capacitor banks

- $\mu_{(v,w)}$: Connection coefficient between point v and w
- β: Set of all Connection coefficients
- V_{min}: Minimum permissible voltage
- V_{max}: Maximum permissible voltage
- $Z_{(v,w)}$: Impedance between point v and w
- V_0: Feeder voltage
- **I**: Identity matrix
- **DLF**: Impedance and connectivity matrix
- $\mathscr{T}$: System topology
- $||V_k||_2$: Voltage Magnitude
- T: V2G schedule stretch
- n: Time slot
- J: Set of EVs preconditioning during T
- I: Set of EVs participating in V2G during T
- $[\delta_i, \Delta_i]$: Availability window of EV i during T
- SoC_i^f: Final SoC of EV i at δ_i
- SoC_i^d: Desired SoC of EV i at Δ_i
- b: Bus number
- k: Number of Buses in the system
- γ_b^n: Available bus b power at during n
- γ: Maximum available power
- $P_b(n)$: Total power load demand on buss b during n
- $L_b(n)$: Base power load demand on bus b during n

- $C_b(n)$: EV charging power load demand on bus b during n
- $D_b(n)$: EV discharging power load injected on bus b during n
- $H_b(n)$: Household power load demand on bus b during n
- a_j^n: Input variable for EV j preconditioning status during n
- ξ_j^b: Input variable for EV j location
- ρ_i^b: Input variable for EV i location
- x_i^n: Decision variable for EV i charging status during n
- y_i^n: Decision variable for EV i discharging status during n

0.3 A Data Driven Performance Analysis Approach for Enhancing the QoS of Public Charging Stations

- SoC: Battery State of Charge
- β: Battery Capacity
- P: Charging power rate
- P_{max}: Maximum charging power rate
- β_t: Threshold battery capacity
- $\mathscr{T}$: Charging time
- β_i: Initial battery capacity
- β_{max}: Maximum battery capacity
- β_r: Requested Battery capacity
- X: Random variable characterizing battery size
- Y: Random variable characterizing initial SoC
- Z: Random variable characterizing requested SoC

- $E[\mathscr{T}]$: Mean charging time
- $V[\mathscr{T}]$: Variance charging time
- λ: Electric vehicles arrival rate
- μ: Service rate
- ρ: system utilization
- L_q: Average number of costumers in the queue
- W_q: Average waiting time in the queue
- Ca^2: Square coefficient of variation of arrival time
- Cs^2: Square coefficient of variation of service time
- p_l: Reneging Probability
- p_j: Probability of having j costumers in the system

Chapter 1

Introduction

1.1 Overview

Recently, the auto industry has seen a paradigm shift towards electric vehicles (EVs) and its production of EVs has accelerated at unprecedented rates. This escalated number of EVs will introduce a colossal changes not only into the transportation sector but also in the power generation and distribution sectors. Consumers' transition to EVs is gaining momentum. The major drivers for this acceleration are the rising awareness by the public for maintaining a clean environment, reducing pollutant emissions, breaking dependencies on oil, as well as tapping into cleaner energy sources. Governments' initiatives to accelerate this transition range from major tax exemptions, lower insurance payments, to convenient parking and fast lanes usage. These numbers reached 7 million passenger EVs in 2019 and are expected to reach 30 million in 2030 [2]. In order to assist globally achieving such ambitious goal, governments are stepping in and pushing their own EV addition targets. For example, the government of Quebec, in Canada expects to reach 1 millions EVs by 2030 [3].

Wistfully, EV adoption is hindered by the driving range anxiety as well as small battery capacities which leads to EV requiring frequent charging. In order to tackle those concerns, governments and power operators are expanding their charging network infrastructure by accelerating the deployment of public Charging Stations (CS) at strategic locations that attract EV users without affecting the performance of the distribution network. Fast DC chargers are being widely considered due to their

beneficial low charging time. Unfortunately, people are still indifferent to using public CSs. For example, Ontario's government of Canada launched a $500 M project to deploy a DC fast charging network in the province. However, after attaining 51% of their objective, it was discovered that most of those stations remain under-utilized [4]. This reluctance in public CS usage is due to users trying to avoid long waiting times and high uncertainty of vacant charging outlet [5].This lead to users favoring private CSs over public ones [5]. Currently, Voltage in Alternating Current (VAC) level 1 and level 2 chargers are available to install at residences and they operate at 120 and 240 VAC with useful power ranging between 1.4 kW and 19.2 kW respectively [6]. EV manufacturers also provide an on-board level 1 charger with each sold EV; hence, level 1 chargers are still the most commonly used in home charging. However, the recent price declination of level 2 chargers [7] [8] has increased its popularity among EV users for daily usage to experience a faster charging rate. As a ramification, within a short period of time, it is expected that a remarkable number of level 1 chargers will be replaced by level 2 chargers at home premises. This increased number of level 2 chargers will come with a remarkable increase in the load on the distribution network, which might result in the network's Quality-of-Service (QoS) degradation. This elevated number of EVs will come with various users' behaviors. Those behaviors will come with various uncertainty and difficult situations for the grid. Mass charging will increase the load dramatically during peak times. Another behavior occurs during cold season to aid users enhancing their EV performance which is preconditioning. Preconditioning will bring additional load during off-peak time. Therefore, EVs' new behaviors such as mass charging and preconditioning that will in turn affect the networks' QoS and power losses which incur monetary losses for the operators.

Accordingly, in this thesis, an extensive study and analysis on the impact of elevated number of EVs and level 2 chargers on the distribution network alongside different behaviors (*i.e.*, mass charging and preconditioning) is performed. Subsequently, a performance analysis of public charging stations with real data is realized, in addition, necessary performance metric are derived to assist EV users in enhancing charging processes.

1.2 Contributions

Multiple concerns arise from the increased number of EVs in today's market coupled with the popularity of home charging using a level 2 charger. The deterioration of the QoS of the power distribution network cause by various users' behaviors still highlight the effects evoked by this shift in the transportation sector. Accordingly, the impact of the increased number of EVs alongside high number of level 2 chargers on the power grid is studied. Extensive analysis and simulations are conducted to examine the effects of mass EV charging coupled with level 2 chargers on the distribution network. Furthermore, the competency of dynamic pricing in holding the network performance metric within operational range is investigated with various charging behaviors.

With the introduction of EVs in such a large number, a new behavior has been observed that can negatively impact the performance of the distribution network that is EV preconditioning. This behavior is coupled with various difficult aspect to the network operators. Hence, the impact of EV preconditioning on the distribution network is studied. Additionally, the capability of network reconfiguration in assisting the network performance is analyzed. Moreover, the elevated number of EVs is leveraged to aid reconfiguration by applying vehicle to grid (V2G) technology in a hybrid method to enhance the network QoS.

The lack of popularity of public CSs led to it being under-utilized. This reluctance is due to not having a proper check-in or reservation system deployed in practice. Therefore, without resorting to approximations, in collaboration with Hydro-Quebec, a data driven charging power and time model is derived that take into consideration the decreasing nature of charging rate during a charging session. Afterwards, the performance of our model is verified with real CS usage data. In order to assist operator enhancing their CS deployment and utilization, based on queuing analysis several CS performance metrics (waiting time, reneging probability and blocking probability) are derived. We verify those metrics by building a discrete event simulators based on parameter from the data to imitate the operation of a CS. In addition, these metrics will also assist users enhancing their charging experience by decreasing the total time spent at such stations and enhance the deployment of stations by operators.

Chapter 2

Impact Analysis of Level 2 EV Chargers on Residential Power Distribution Grids

2.1 Introduction

The transition from level 1 to level 2 may have a drastic turnaround in the distribution grid's load profile, which may result in disturbances and in worst cases a blackout. As reported by a study in Lisbon, Portugal, 10% of the total EVs' penetration to the power grid is enough to drop its voltage level significantly if charged at peak times [9]. Hence, with the target of 1 million EVs by 2030 in Quebec [3], a large number of level 2 chargers will be deployed and will dominate the residential load profile. As a ramification, the existing power distribution network may fail to serve peak demand. In this work, we will conduct extensive analysis and simulations to evaluate the impact of this increased number of level 2 chargers, and have a better understanding of the forthcoming consequences. Moreover, we will evaluate the proposed dynamic pricing solution in presence of high number of level 2 chargers and a randomized EV charging behavior. In our work, we simulate real-life scenarios, where EVs are categorized according to their battery size. In addition, we study the effect of multiple penetration rates of level 2 chargers along with an expected penetration growth of EVs, with implementing a ToU and ToP (Time-of-Peak) pricing technique with different EV charging behavior (i.e., charging behavior may be influenced by different pricing techniques). We use power-flow equations to measure the voltage level of different buses of the residential power

distribution network and hence, analyze the effect of EV charging. Based on the charging behavior, we investigate the competency of different pricing techniques to mitigate this impact. Our goal is to illustrate the upcoming complications to the power distribution network caused by increased number of EVs and level 2 chargers, as well as assess the competency of suggested countermeasures.[1]. The remainder of this chapter is organized as follows. Section 2.2 presents related work. The EV charging system is covered in Section 2.3. Section 2.5 details our simulation's environment. We present our simulation results in section 2.6. In Section 2.7 we conclude this chapter.

2.2 Related work

The impact of large scale EV penetration has also caught the attention of both academia and energy provider companies. Several studies have been conducted to enhance the experience of owning and charging EVs without disturbing the electrical grid. The authors in [11] studied the impact of charging Plug-In Hybrid Electric Vehicles (PHEV) on a residential distribution grid in terms of power losses and voltage deviations. In addition, they showed the difference between coordinated and uncoordinated charging of PHEV. However, they only considered PHEV in their analysis. The authors in [11] did not take into consideration Battery Electric Vehicle (BEV) that have larger batteries compared to PHEV. On the other hand, the work of [12] revolved around the concept of understanding how does residential EVs affect the distribution system voltages. The authors only considered level 1 chargers in their simulation in addition to assuming constant battery size for EVs. They proposed a controlled charging scheme with Time of Use (ToU) pricing techniques to mitigate the effect of mass charging. In [13], the authors studied the impact of single-phase charging strategies on the residential grid, disregarding the elevated number of level 2 chargers. While the authors in [14] studied the repercussion of elevated number of EVs in a residential area and their effect on the distribution grid. In their work, the authors assumed only level 1 chargers and a constant charging time for all EVs. Furthermore, they evaluated ToU pricing technique as a solution to avoid elevated peak caused by the increased number of EVs, assuming all EVs will adapt the proposed pricing scheme. The performed studies in the literature agree that an elevated number

[1]This work has been presented at the IEEE CPE Power Engineering Conference 2020 [10]

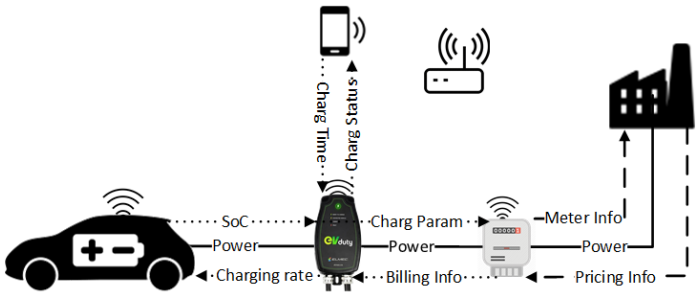

Figure 2.1: An example of a private CS.

of EVs can disturb the power distribution network especially with the shift towards the use of level 2 chargers.

2.3 EV Charging System

At present, EV charging systems can be categorized in two categories: public and private charging stations (CS). Public CS include parking lots at work spaces and shopping malls equipped with an EVSE (Electric Vehicle Supply Equipment) to offer charging services to employees and visitors. On a regular basis, employee and shopping center visitors spend enough time to conduct a long charging procedure or discharge to offer ancillary services for the grid. Furthermore, commercial operators or power distributors are installing dedicated charging stations on public roads and lands, similar to petrol stations, to offer charging services for EV users on the go.

Private CSs are the ones deployed at residential premises. Those consist of an EVSE connected to the house's smart meter. EVSEs can be enabled with a smart controller to allow user connection through the Internet or a mobile application. This facilitates the management of the charging and billing process. A sketch of a private CS is presented in Fig. 2.1 where several parameters are exchanged between the entities to start/stop the charging process. Currently, the market offers three levels of chargers: levels 1, 2 are AC chargers while level 3 is a DC fast charger. AC chargers are usually used for private CS. In this work, we only consider residence charging scenarios with level 1 and 2 chargers, since these are the ones that might degrade the voltage level of residential distribution grid [6].

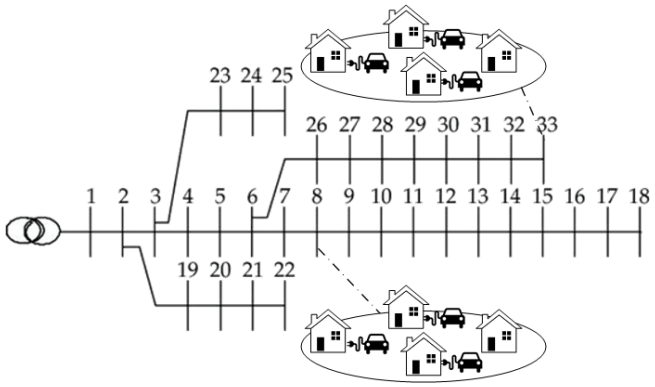

Figure 2.2: An example of residential distribution network.

2.4 System Model

The aim of this work is to have a better understanding of the impact imposed by the elevated adoption rate of EVs with an increased deployment of level 2 chargers on the residential distribution network. For that purpose, we will build our system around the IEEE-33 bus radial distribution standard as shown in Fig.2.2.

The residences are assumed to be uniformly distributed among the buses. EV charging requests can be initiated at every residence depending on the penetration rate of EVs. The arrival of one charging request does not provide any information about future requests, as a result, due to it's memory-less property, the exponential distribution serves as a best model for the inter-arrival time of requests following Equation 2.1. Respectively, the request arrival follows a Poisson arrival process.

$$f(x,\lambda) = \begin{cases} \lambda e^{-\lambda x} & \text{if } x \geq 0 \\ 0 & \text{if } x < 0 \end{cases} \tag{2.1}$$

We model our system over 24hrs and each hour is considered as a single time slot. The request arrival rate (λ) is assumed to have a certain distribution according to the type of day, for example, in weekdays λ is higher during peak time where users comes back from work as depicted in Fig. 2.3 [15]. Each request has different charging rate depending on whether it is attached to a level 1 or level 2 charger, where each level has a penetration rate that each request is going to be assigned according to this rate.

Table 2.1: Electric Vehicles Categories.

Category	X-Small Battery	Large Battery	Medium Battery	Small Battery
Max Battery size (kWh)	18.8	100	64	35.8
Min Battery size (kWh)	4.4	50	39.2	16.7
Average Battery Size (kWh)	10.8	77	51	26.33
STD Battery size (kWh)	3.8	20	11.9	7.5
Ratio over total EVs (%)	51.7	10.7	25.8	11.8

EVs are divided into four categories based on their battery size: large battery, medium battery, small battery, and Extra-Small battery (PHEV). Each request is drawn from the distribution of the latter four categories [16]. Each category of EVs has its own battery size, β (Min, Max, Std, and average) modeled from the data acquired from [16]. We select the State-of-Charge (SoC) of a charging request, as the required power to have a full battery, following a truncated normal distribution [17] using the parameters shown in Table 2.1. Charging time for each request is calculated using equation 2.2:

$$T = \frac{SoC * \beta}{\zeta} \tag{2.2}$$

where ζ represents the charging rate. In our formulation, we consider three different pricing models, Static, ToU and ToP to assess their competencies over maintaining bus voltage stability based on the charging behavior of EV users. The static pricing model is independent of time or load where the consumer is billed according to a flat rate. This model renders the charging behavior of EVs indifferent. To escape charging during peak load hours, power distributors deploy ToU or ToP pricing mechanism. In a ToU pricing model, the usage is rated differently according to when the service was used, during peak or off-peak hours (lower-rate). Through ToU, users are persuaded to initiate charging procedures during off-peak hours. On the other hand, ToP policy increases the pricing rate once the user passes a certain load threshold [18] [19]. According to the literature, [14, 20], implementing ToU is advantageous for demand-side management schemes. Nevertheless, in our study, we will evaluate both ToU and ToP in the presence of increased EV and level 2 chargers adoption.

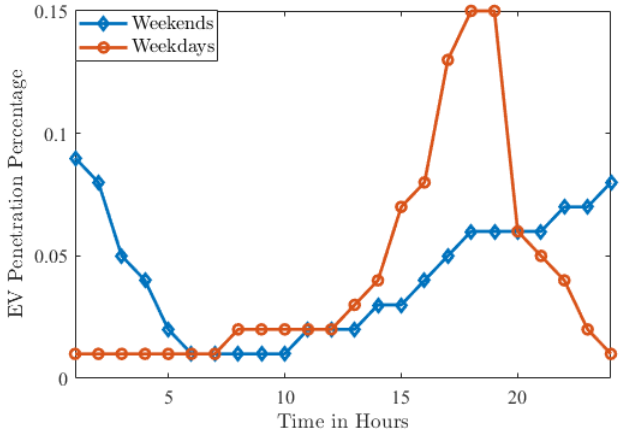

Figure 2.3: EV's Charging request percentage distribution.

2.5 Simulation Environment

To analyze the impact of increased level 2 charger adoption in the presence of large scale EV penetration at power distribution grids, we build a PYTHON base discrete event simulator. We design the simulator to work in two stages with a slotted timeline of 24 one hour slots. An image of the IEEE-33 Bus system is built into the simulator [21], and the number of residences is uniformly divided upon the buses of the network. In addition, each residence has its own base daily load that is registered without the presence of EV [21].

In the first stage, we establish an arriving process of charging requests with a variable arrival rate according to the corresponding time slot as depicted in Fig. 2.3. Each arrival is assigned a level 1 or 2 charger following the penetration rate of level 2 chargers at customer residence. Moreover, EV and SoC are selected as outlined in Section 2.4. Afterwards, we calculate the charging time per request using equation 3.2.

In order to simulate a real-life scenario, we assign a charging deadline drawn from a truncated Gaussian distribution [17] to each request. The charging process is terminated as per this deadline regardless of the SoC. Ultimately, EV load is recorded and added to the base load of the corresponding residence. In the second stage of the simulation, a power-flow equations are solved, using Newton-Rapson method. These equations utilize the real power, reactive power, and voltage magnitude at the sending end of a branch to express the same quantities at the receiving end of the branch.

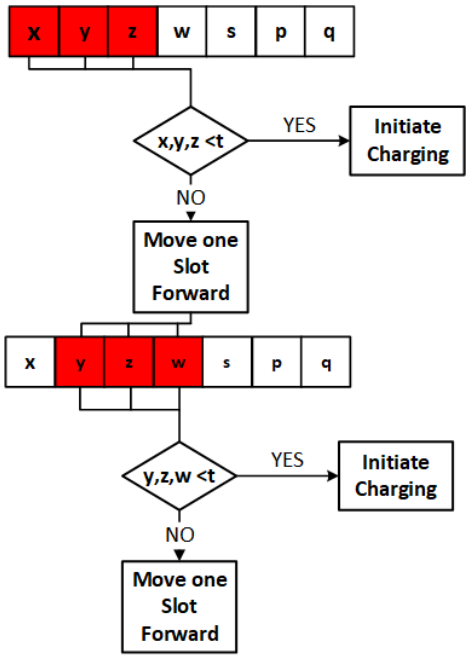

Figure 2.4: Flow chart of charging procedure for Eco charging behavior.

This method is utilized to measure the voltage level at each bus of the system following equation 2.3 [22]:

$$V_{n+1}^2 = V_n^2 - 2(r_n P_n + x_n Q_n) + \frac{(r_n^2 + x_n^2)(P_n^2 + Q_n^2)}{V_n^2} \tag{2.3}$$

where:

- V_{n+1} : Voltage of bus $n+1$.
- V_n : Voltage of bus n
- P_n : Active power flow from bus n to $n+1$
- Q_n : Reactive power flow from bus n to $n+1$
- r_n : Line resistance between bus n and $n+1$
- x_n : Line reactance between bus n and $n+1$

Furthermore, three charging behaviors are implemented in the simulation [23]:

- *Greedy*: where charging requests are immediately initiated upon arrival.

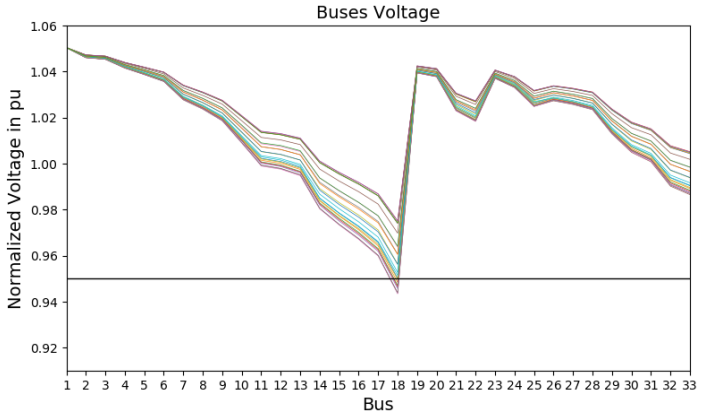

Figure 2.5: Normalized Buses Voltage (pu.) for static pricing, $\alpha = 50\%$, $\sigma = 50\%$.

- *Eco*: where the user observes the pricing of three consecutive slots. If the prices are below a certain threshold, charging is initialized. If not, the user will shift his observation one slot forward. The flow chart shown in Fig. 2.4 describes this behavior. The EV user checks first three consecutive slots (x, y, z) and if all these slots show a price less than a threshold value, t, the user EV will start charging; otherwise, the user will check (y, z, w) and so on.

- *Half-Eco*: if deadline is less than the required charging time, the Greedy approach is selected, otherwise it will follow the Eco approach.

2.6 Results and discussions

In order to study the effect of increasing tendency of using level 2 chargers for EV charging at residences, we simulate various scenarios for different adoption rates. Furthermore, we evaluate the competency of two different dynamic pricing mechanisms.

Initially, we set-up the environment described in section 2.5, with constant parameters such as number of residences, R and EVs adoption rate, α. The EVs adoption rate, α is set with respect to residence numbers, R (these R number of houses are uniformly distributed among all buses). The ratio of different types of EVs shown in Table 2.1 is taken as an input to generate the EV arrival requests. Afterwards, each request is assigned an SoC drawn from a truncated Gaussian distribution following the given parameters of Table 2.1. For each request, we generate a deadline following a truncated Gaussian distribution with a maximum of 16 hours and minimum of 4 hours to imitate the

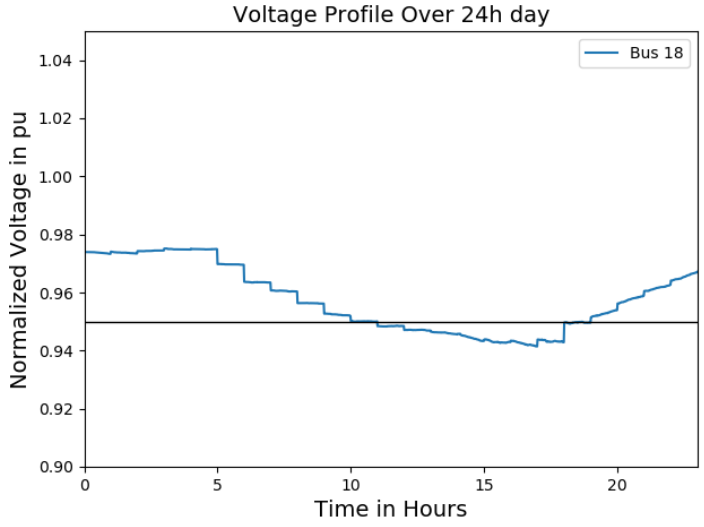

Figure 2.6: Bus 18 voltage profile with static pricing, α = 50%, σ = 50%.

amount of time spent inside a house. We also consider a level 2 charger adoption rate σ to represent how many EV users utilize level 2 chargers at their home to charge EVs.

We run our simulation with 10000 residences and a different values of EV penetration (e.g., $\alpha =$ 20%, $\alpha = 50\%$, $\alpha = 80\%$ etc.). We also vary σ, the level 2 chargers adoption rate. Each EV charging request arrival is assigned a category following the ratio presented in Table 2.1.

First, we analyze the impact of level 2 chargers penetration in the presence of a static pricing mechanism. As in static pricing the price is not varied with time or consumption, EV users are considered to have a greedy behavior, and thus each charging process is initiated upon arrival. Originally we simulate weekdays scenario, Fig. 2.5 depicts the normalized bus voltages for the 24 time slots (each line represent one time slot [1 hr]) for $\alpha = 50\%$ and $\sigma = 50\%$. We notice that the network fails to adopt the imposed load on it, since the voltage drop below the acceptable threshold (0.95 pu) for bus 18 at some time slots. In order to investigate the severity of the elevated load, Fig. 2.6, depicts the 24 hrs voltage profile for Bus 18 with the static pricing for the same value of α and σ. As shown in Fig. 2.6, the readings collected from Bus 18 indicate a voltage drop below 0.95 pu during peak hours. This drop is due to the negative impact of the EV load on the distribution network. Most power distributors apply static pricing as their current network setting. In order to evaluate the response of those settings under the stress of elevated EV adoption and high number of level 2, for that matter, in Fig. 2.7 we depict bus 18's voltage level for different adoption rate in function of

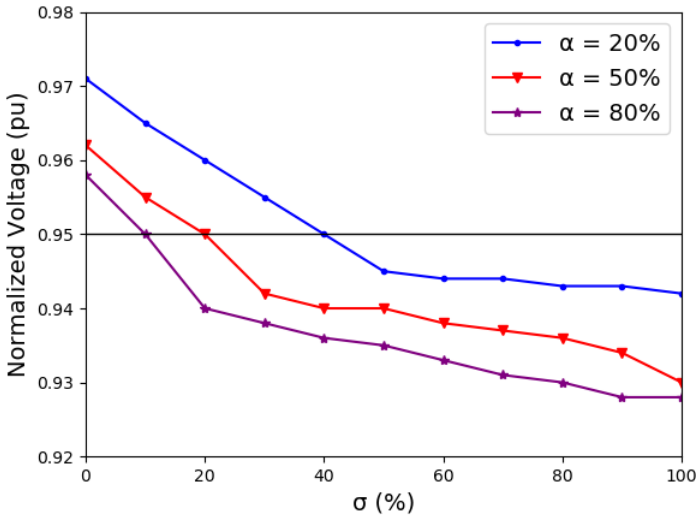

Figure 2.7: Normalized voltage level for bus 18 during peak time (16:00).

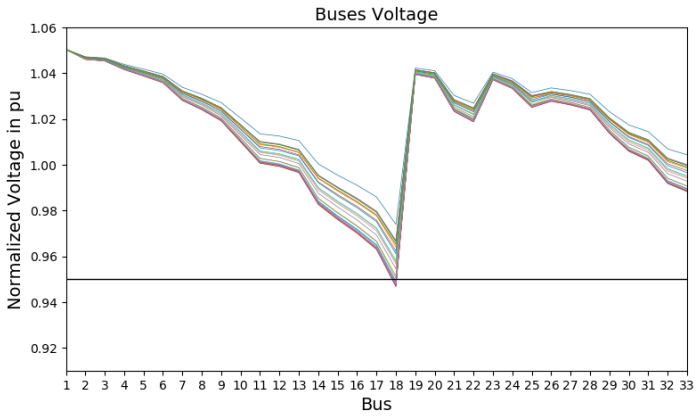

Figure 2.8: Normalized buses voltage for ToU, $\alpha = 50\%$, $\sigma = 50\%$.

level 2 switching rate. We notice this setting under-perform when the number of level 2 charger is high with an elevated EV penetration.

Next we evaluate the competency of ToU to maintain the voltage level over the threshold with the increased adoption rate of level 2 chargers. As mentioned before, level 2 chargers require a smaller charging time at a higher rate which may cause a surge on the network. To investigate this scenario, we assume that 50% of users are adopting half economic behavior while the rest is 25% Full-Eco and 25% greedy. The outcome of this scenario is shown in Fig. 2.8, where we notice that ToU is able to decrease the voltage drop of bus 18 by roughly 2% at peak time. However, the network still experiences a voltage drop below 0.95 pu. Moreover, Fig. 2.9 shows that the voltage

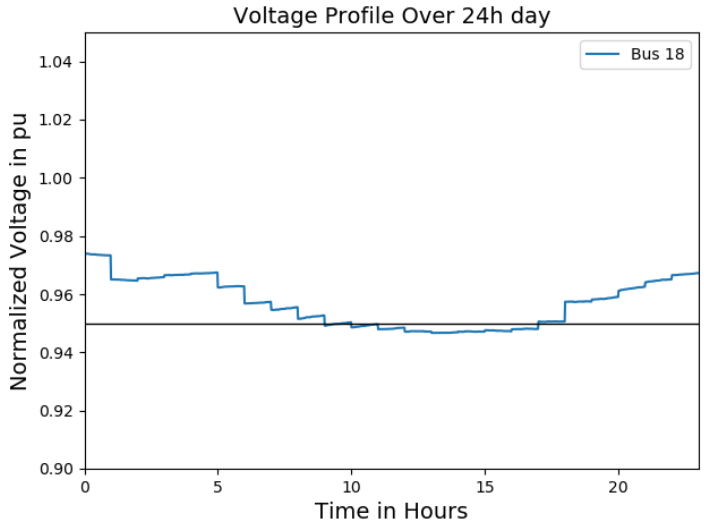

Figure 2.9: Bus 18 voltage profile for ToU, α = 50%, σ = 50%.

drop is shifted slightly toward the off-peak times; that means more load is shifted to off-peak time as illustrated in Fig. 2.10. As utility providers usually forecasts the demand of each area in order to generate enough power to support this demand, they may face issues when a new load peak arise in an off-peak time.

Furthermore, we evaluate another comparatively less applied pricing mechanism, ToP, where each user aims at maintaining a minimum power bill. As a ramification, a large number of users may initiate their charging at the same time if they are adopting the same charging behavior. To assess the situation, we assume that 50% of users adopt the Half-eco and 25% Full-eco and 25% greedy. From Fig. 2.11, we notice that ToP can improve the voltage level of bus 18 by almost 2% at peak time compared to static pricing, but still this is not adequate enough to maintain the threshold level. On the other hand, Fig. 2.12 shows a load shift to off-peak and may lead to similar consequences as ToU.

As we expect a different load profile during weekends (comparatively a lower arrival rate is expected at peak hour), we evaluate the outcome of these three different pricing mechanisms and their impact on maintaining voltage level. However, even for a weekend, we notice a disturbance to the grid for the same penetration rate of EVs and level 2 chargers 2.13 (α=50% and σ=50%) as shown in Fig. 2.13. Finally, we can conclude that though dynamic pricing is able to shift a portion of load from peak to off-peak time, this is not enough to maintain the minimum voltage level with

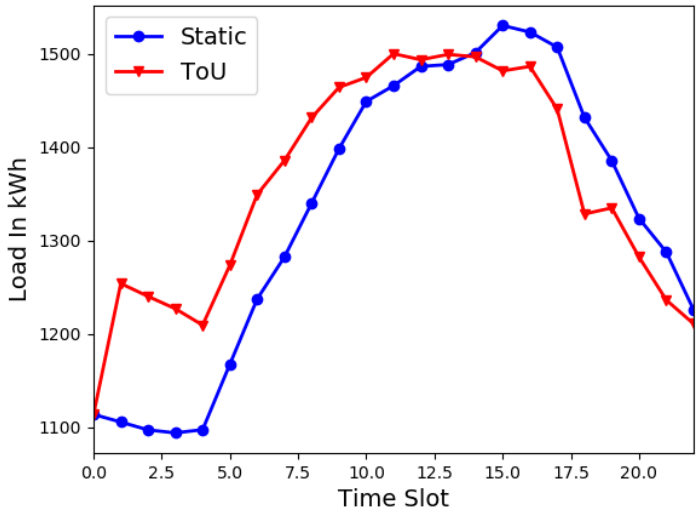

Figure 2.10: Load profile with $\alpha = 50\%$, $\sigma = 50\%$.

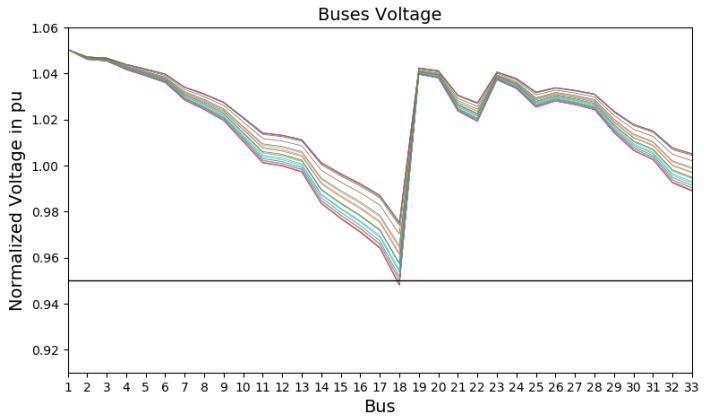

Figure 2.11: Normalized Buses Voltage for ToP, $\alpha = 50\%$, $\sigma = 50\%$.

the burgeoning tendency of installing level 2 chargers at residential areas.

2.7 Conclusion

In this chapter, we designed and built a discrete event simulator to imitate real-life EV mass charging in residential areas and assess the impact of the increased adoption rate of level 2 chargers on bus voltage. The collected results through simulation confirmed that a challenge to accommodate load from level 2 chargers awaits utilities at the distribution network level. We characterized this challenge as a failure to maintain a minimum voltage level (0.95 pu), especially at peak times. Furthermore, we evaluated the applicability of different pricing mechanisms present in the literature

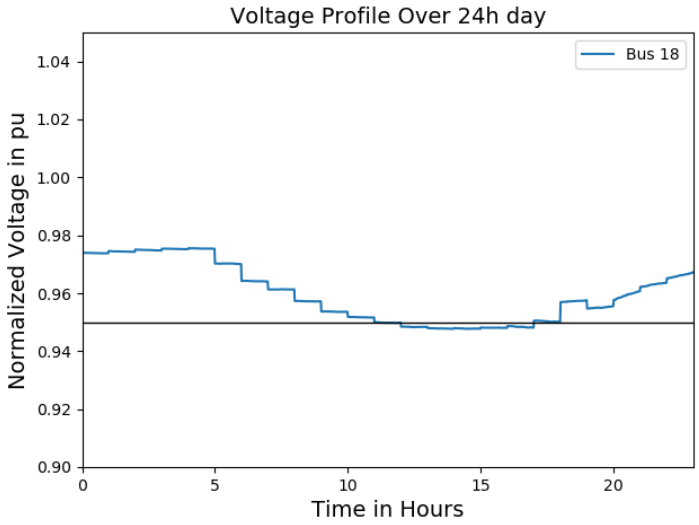

Figure 2.12: Bus 18 Voltage Profile (pu.) with ToP, α = 50%, σ = 50%.

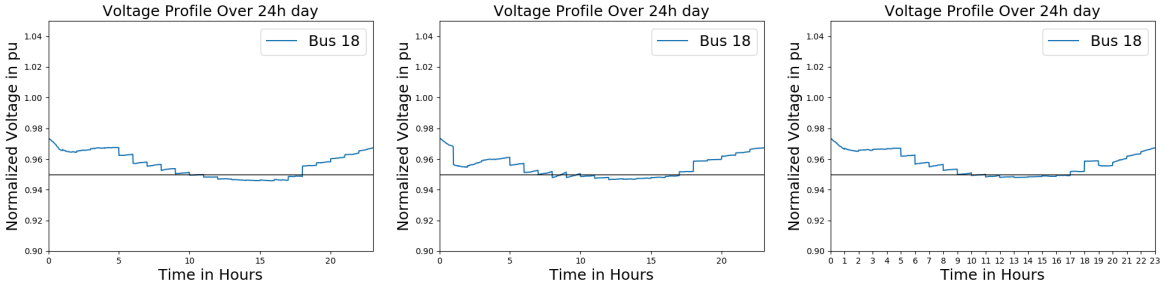

(a) Static Pricing. (b) ToU. (c) ToP

Figure 2.13: Weekends normalized voltage profile (pu.) for α=50% σ= 50%.

and their impact on maintaining the required voltage level. Our simulations demonstrated that those mechanisms are not enough to ameliorate the impact of large scale level 2 charger penetration. Thus, there is a need for more advanced solutions in the form of smart scheduling and dynamic pricing. We aim at investigating and developing those solutions as part of our future work.

Chapter 3

Assisting Residential Distribution Grids in Overcoming Large Scale EV Preconditioning Load

3.1 Introduction

We demonstrated in chapter 2 that an elevated number of EVs alongside side a high number of level 2 chargers can have a negative impact on the performance of the distribution network. To alleviate the impact (e.g., voltage degradation, power loss, etc) of such expected peak load, operators can resort to different peak shaving techniques. For example, imposing dynamic pricing to encourage EV users to charge during off-peak hours [14], intelligent scheduling of EVs for flattening the load curve [24] or reconfiguring the network to minimize energy losses [25]. Moreover distributed energy sources, especially Vehicle-to-Gird (V2G) technology [26] can also be implemented to compensate for the abrupt demand. Regardless of the implemented peak shaving technique, the action is load shifting from peak to off-peak (e.g., early morning). Consequently, peak shaving methodologies increase the load during off-peak, and such load can be significantly increased during winter due to the higher usage of water heaters and heating systems [27]. During winter periods, this off-peak

load can also start to exhibit inclining behavior due to EV users' tendency to precondition their vehicles before leaving their residences. Preconditioning process in internal combustion engine (ICE) vehicle corresponds to heat the passenger cabin and engine block, while in EV paradigm it heats the cabin and the battery compartment [28]. Since preconditioning enhances the performance of EVs and increases its range during cold weather [29], most newly manufactured EVs are equipped with the option of cabin and battery compartment preconditioning to persuade people into purchasing an EV [28], [30]. A survey over ICE vehicle users in Quebec depicts that 32.9% of daily car users, and 27.4% of frequently car users, warm up their vehicles using remote starters [31]; accordingly, it is also expected that the upcoming large number of EVs will be engaged in preconditioning process during winter while plugged in their home chargers to alleviate some of their range anxiety [28]. The capability of simultaneous charging and preconditioning of level 2 charger [28] and its declining price elevate the number of level 2 chargers in residential premises, which may render preconditioning a potential threat to the distribution network. The National Household Travel Survey (NHTS), conducted by the Federal Highway Administration (FHWA) [32], shows an increment in the daily trips initiated between 6 AM and 9 AM, the period when people usually leave their houses to work. Preconditioning takes 20 to 30 minutes [28], [30] before EV users leave their houses during winter time; thus, a surge of electric demand is expected to be added onto the grid to cater this large number of EVs and their preconditioning. Compared with EV charging process, EV preconditioning occurs over a shorter period with a more imminent deadline; hence, existing peak shaving techniques might not be suitable to maintain the power quality during the mass preconditioning period. Indeed, EV charging was found to be somewhat troublesome due to the fact that users demand more control over the process [33], thus with a shorter duration, preconditioning becomes a more challenging problem. In this chapter, we analyze the impact (i.e., voltage degradation and power loss) of large scale EV preconditioning on the grid and demonstrate the limitations of load shaving mechanisms in mitigating this impact. We first apply network reconfiguration and assess its competency to handle the abrupt demand of preconditioning. Though the performance of network reconfiguration in maintaining threshold voltage level or minimizing power loss is supposed to be degraded with the increased number of EVs, the large number of EVs offers an opportunity to compensate the abrupt

demand by discharging energy from EVs via V2G technology. Hence, we also investigate the applicability of V2G, wherein EVs that are not bound to leave the premises shortly (hence, are not part of the EV preconditioning load) can participate by supplying energy to other EVs, subject to having their batteries recharged by their own deadlines. Finally, to achieve a better solution, we propose and evaluate a hybrid model where both techniques, reconfiguration and V2G, can be leveraged to mitigate the dire consequences of large scale EV preconditioning. [1] The rest of the chapter is organized as follows: in Section 3.2, we present the literature review while in Section 3.3, we present the impact of EV preconditioning on the residential distribution network. Section 3.4 presents different load balancing techniques and in Section 3.5, we present our simulation results and discussion. Finally, in Section 3.6, we conclude the chapter.

3.2 Literature Review

As per our knowledge preconditioning has not yet been considered as a potential distribution network service deterioration, since charging is mainly conducted with level 1 chargers. However, with the increasing number of level 2 chargers at residential areas, preconditioning renders itself a probable impairment on the distribution network with an additive load during off-peak times. Various techniques were studied as an attempt to regulate the load profile and decrease the peak power demand. Applying dynamic pricing, such as Time-of-Use (ToU), has been investigated as a promising approach to shape the peak load of distribution networks. The advantages of implementing ToU for demand-side management schemes was inspected by shifting EV charging more towards off-peak times [14, 20]. A scheduling scheme for demand side management and Home Energy Management System (HEMS) was devised in [35], where an energy company sends a pricing signal based on a hybrid day ahead real-time pricing and inclines block pricing. Moreover, the consumption of several appliances was scheduled to ensure lowest tariffs over a period of a single day. The work of [36] revolved around devising a Mixed Integer Linear Program (MILP) for HEMS management under different pricing and power-limiting techniques, such as, demand response, PV

[1] Part of this work [34] is accepted and will be presented at IEEE SmartGridComm'2020.

operation, distributed generations and Vehicle to Grid (V2G). Radial distribution network reconfiguration was investigated in [25] as a load balancing and loss reduction technique. Generally speaking, these techniques modify the system topology using tie-switches and sectionalizers to ensure its radial connectivity as well as achieve an improvement in terms of performance. An extensive review of the existing literature for network reconfiguration approaches was discussed in [37]. Vehicle to grid (V2G) transfer capability of EVs might be considered as another auxiliary solution for peak shaving. The use of batteries in EV structure enables V2G technology and renders EVs charging and discharging operation a feasible solution to reduce peak load demand. In [38], a feasibility study for V2G with Plug-in Hybrid Electric Vehicles (PHEV) was conducted to determine the number and energy capacity and charging operation of PHEV to ensure the best outcome from V2G. The authors of [26] suggested an adequate approach to utilize EV's batteries to reduce the peak load demand using a dynamic discharge rate. The work of [39] revolved around optimizing the PHEV charging schedule to take advantage of excess wind energy and utilize V2G strategy to keep the total load demand below certain limit. However, the randomness of EV positions and availability rendered their usage as a potential peak shaving solution troublesome. In [40] the authors propose a blockchain-based secure energy trading environment to secure incentive contracts between users and operators. In addition, their environment is assisted by edge computing offloading to ensure block creation.

While not too much work addressed the preconditioning process of EVs, the impact of the upcoming high number of EVs on the Estonian distribution number was analyzed in [41]. In their work, the authors considers preconditioning as a regular short charging period without considering the nearly identical deadline for such process on the grid. In this work, we will first analyze the impact (e.g., voltage degradation, power loss, etc) of preconditioning on the distribution network under various penetration rates and different scenarios of EV charging. In addition, we will investigate various mitigation techniques for load balancing and loss reduction in distribution networks and their effectiveness on EV preconditioning and finally depicts a hybrid approach to handle this upcoming load.

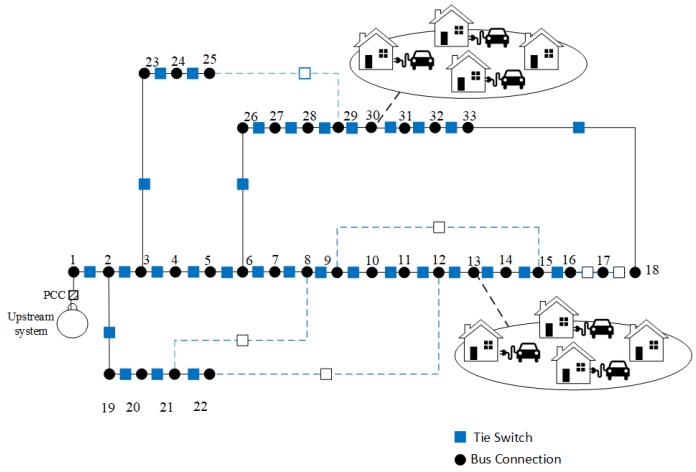

Figure 3.1: An example of residential distribution network.

3.3 Impact Analysis of EV preconditioning

3.3.1 Adopted System Model

EV Charging

We devise our EV charging model following our work in chapter 2, where we use the IEEE-33 radial bus distribution system [42]. Each bus has a nominal winter residential load [43], and residences are uniformly distributed over the system as depicted in Fig. 3.1. EV charging requests are initiated at residence following EV penetration rate α. In addition, we adopt the exponential distribution to approximate EV charging request inter-arrival time following Eq. (3.1), where λ is charging requests arrival rate. Respectively, EV charging requests follow a Poisson arrival process.

$$f(x,\lambda) = \begin{cases} \lambda e^{-\lambda x} & \text{if } x \geq 0 \\ 0 & \text{if } x < 0 \end{cases} \tag{3.1}$$

We divide the timeline into 24-one-hour time slots. Charging requests arrival rate λ is variable for each time slot and assumed to follow a certain distribution with higher rates during peak hours as depicted in Fig. 3.2 [15]. In addition, each request is attached to a level 1 or 2 charger according to level 2 adoption rate σ, and a battery capacity depending on its category [44]. Finally, we assume that each arriving EV have a random State-of-Charge (SoC) drawn from a truncated normal

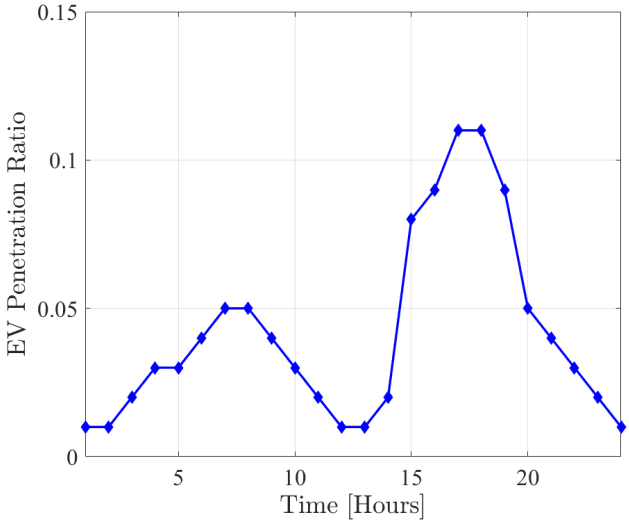

Figure 3.2: EV arrivals percentage during a weekday.

distribution and require to be charged to reach a 100% *SoC*. Required charging time for each request is then calculated following eq. (3.2):

$$\tau = \frac{SoC * \Phi}{\zeta} \tag{3.2}$$

where ζ is the charging rate and Φ is the battery capacity.

EV Preconditioning Model

We assume some EVs attached to a level 2 charger will initiate preconditioning requests during the morning window (5 to 10 AM). Similar to charging requests, preconditioning requests arrival are assumed to follow a Poisson arrival process with variable arrival rate π, as shown in Fig. 3.3. Each request is assigned a duration following the truncated normal distribution, where the power drawn from the grid during this duration is constant to a level 2 charger rate since preconditioning is more beneficial with a level 2 charger [45].

Once the load profiles are populated, we need to calculate the voltage level at each node (Bus) of the system. Therefore, we apply power flow for the generated load profiles in order to obtain bus voltage level, once the bus voltage is known, we use it to determine the system losses [46].

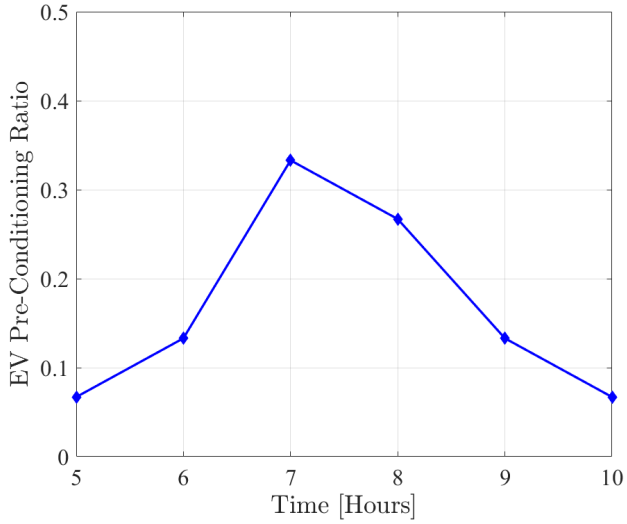

Figure 3.3: EV preconditioning Percentage.

3.3.2 Study of the Impact - Results

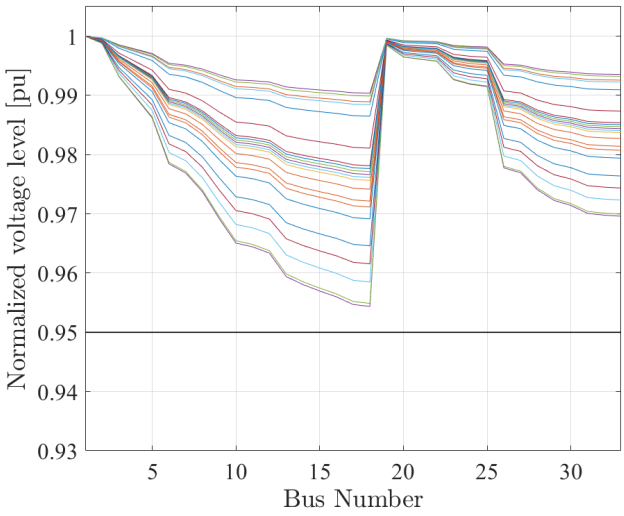

Figure 3.4: System voltage initial settings.

We first present the performance of our system under normal conditions; therefore, in figure 3.4 we depict the system voltage level without the presence of mass EV charging or preconditioning. We observe that our system is able to handle the load imposed on it under initial condition.

Subsequently, to demonstrate the consequences that preconditioning may impose on the distribution network, various simulation scenarios are performed using a python discrete event simulator to

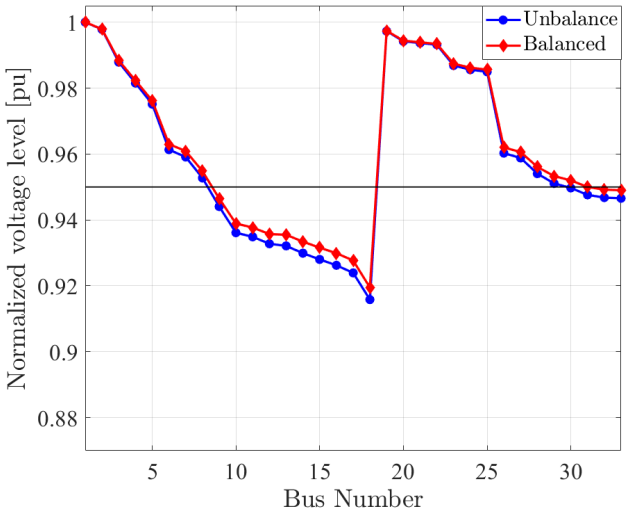

Figure 3.5: system voltage level comparison: $\alpha = 50\%$ & $\sigma = 50\%$ 8 AM.

generate the load profile. In the first step of the simulation, we populate the EV charging requests on top of a nominal load. Afterwards, we generate preconditioning processes that will be conducted during the morning hours. In our simulation we adopt static pricing (flat rate) where users will follow a greedy behavior for charging and preconditioning. Once we generate load profiles, we feed them into a power system analysis software package (MATPOWER) [47] to perform power flow calculation to get the voltage magnitude and total real system power losses.

We first simulate the scenario where we have 50% EV penetration rate (α) and 50% level 2 switch rate (σ) where 80% of those using level 2 will initiate a preconditioning process during the morning time. In Fig. 3.6 we depict the system voltage level, we notice that during some morning time slots the voltage level drops below the acceptable operating threshold (0.95 p.u.). In order to compensate for this voltage drop, operators will inject more power into the network. In Fig. 3.7, we observe that the during preconditioning window the losses are increased, which will impose monetary losses for the utility in response to injecting more power into the system [48]. In order to understand the performance of different systems, we solve for the same scenario of a single time slot the power flow for an unbalanced phases system architecture. In figure 3.5 we depict the voltage level comparison between balanced and unbalanced systems at 8 AM. We notice that both systems have similar performance under the stress of EV preconditioning. Therefore, for the rest of the chapter will be

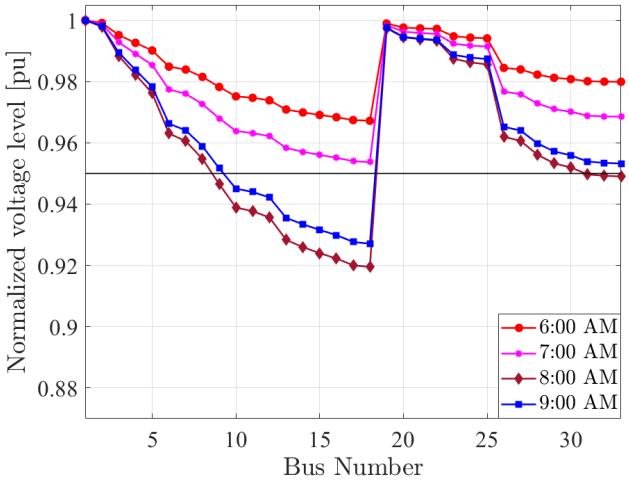

Figure 3.6: System voltage level: $\alpha = 50\%$ & $\sigma = 50\%$.

only considering balanced system.

In Fig. 3.8, we illustrate the system voltage level for an elevated number of EVs and increased number of level 2 chargers (both α and σ are 80%). We notice for the forthcoming EV and level 2 load along side preconditioning, the voltage drop is more severe and affect more time slots during the preconditioning window. Again Fig. 3.9 depicts the power losses over the system, where we notice again an increase in the power losses. Hence, from this analysis, it can be deduced that EV preconditioning is going to add a negative impact in terms of voltage degradation and power loss on residential grids and these consequences would be more severe with a higher penetration of EVs and with larger level 2 charger adoption, which is actually inevitable for the sake of curtailing GHG emission. As a consequence, a set of mitigation methods are investigated to handle these consequences.

3.4 Mitigation Methods

To minimize the power loss due to the abrupt demand by EV preconditioning and to maintain the voltage level of each bus of the system over an acceptable threshold (0.95 p.u.), we propose a combination of network reconfiguration (NR) and energy supply through vehicle to grid (V2G) processes, which are described in the sequel. Both together can be used as a mitigation for the new

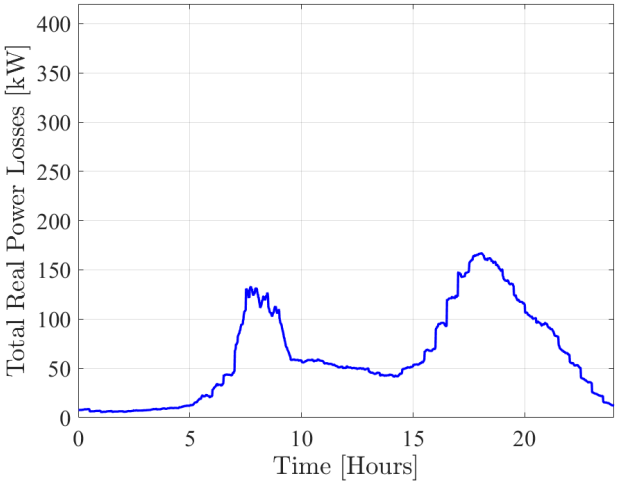

Figure 3.7: Total real system power loss: $\alpha = 50\%$ & $\sigma = 50\%$.

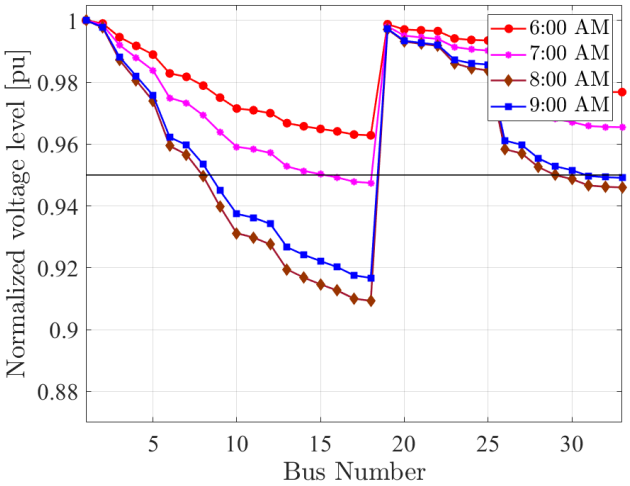

Figure 3.8: System voltage: $\alpha = \sigma = 80\%$.

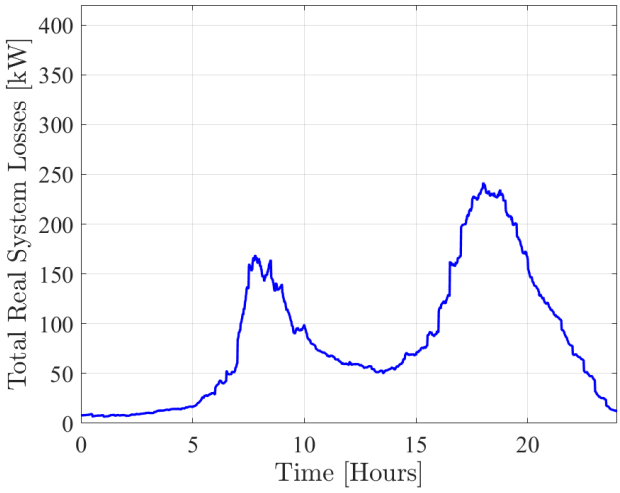

Figure 3.9: Total real system power loss: $\alpha = \sigma = 80\%$.

load arising from preconditioning. We consider a preconditioning period (e.g., morning from 6AM-9AM) and assume a time slotted system where at each one hour time slot, there is a preconditioning demand. We describe first the reconfiguration and then elaborate our V2G mitigation model.

3.4.1 NR for Mitigating Preconditioning Load

Network reconfiguration has been proposed as a load balancing and power loss reduction technique for radial distribution systems [25]. The reconfiguration of a distribution grid often refers to selecting a new radial topology for the system by connecting/disconnecting a set of tie-switches sectionlizers based on an optimization algorithm. This algorithm can be designed to improve various characteristics of system operation such as loss reduction, voltage regulation, cost efficiency, etc. The system power losses is calculated as follows:

$$P_{loss} = P_{feeder} - \sum_{i=1}^{N_L} P_{load} - \sum_{i=1}^{N_{EV}} P_{EV} \tag{3.3a}$$

$$Q_{loss} = Q_{feeder} - \sum_{i=1}^{N_L} Q_{load} - \sum_{i=1}^{N_{EV}} Q_{EV} - \sum_{i=1}^{N_C} Q_C \tag{3.3b}$$

where N_{EV}, N_L, and N_C are the number of EVs, loads, and capacitor banks, respectively. P_{loss} and Q_{loss} represent the loss in the system, and P_{feeder} and Q_{feeder} indicate the active and reactive power

that enters the distribution system, respectively. Reconfiguration problems are often formulated as a minimization of an objective function that account for loss, cost, voltage deviation etc. Without loss of generality, it is assumed that the main aim of the system reconfiguration is to minimize the loss of the system as:

$$Min \quad \mu_{(v,w)} Z_{(v,w)} |I_{(v,w)}|^2 \quad \forall v,w \in N \; \mu_{(v,w)} \in \{1,0\} \tag{3.4}$$

s.t.

$$\mathbf{V} = V_0 \mathbf{I} + [\mathbf{DLF}(\mathscr{T})]\mathbf{I} \tag{3.5a}$$

$$\{\mu_{(v,w)}\} \notin \beta \tag{3.5b}$$

$$V_{min} \leq ||V_k||_2 \leq V_{max} \tag{3.5c}$$

where the connection coefficient ($\mu_{(v,w)} \in \{0,1\}$) determines whether a line is connected between point v and w ($\mu_{(v,w)} = 1$) or not ($\mu_{(v,w)} = 0$), β is the set of all connection coefficients that provide a loop in the distribution system, and V_{max} and V_{min} indicate the maximum and minimum permissible voltage of MV grid, respectively. In addition, $Z_{(v,w)}$ represent the impedance between point v and w, V_0 is the voltage at the distribution substation multiplied with the eye matrix $\mathbf{I}$. **DLF** is a matrix that shows the connectivity and impedance of the nodes together, $\mathscr{T}$ represent the topology of the system that we are on. Finally, $||V_k||_2$ is the voltage magnitude [49].

3.4.2 V2G for Mitigating Preconditioning Load

Another mitigation technique is to rely on EVs that may be willing to cooperate in aiding the network by discharging through V2G technology. V2G has shown to be a good potential load balancing assistant scheme [50]. However, users' might be hesitant to allow V2G on their vehicles due to fear of leaving with low *SoC*, battery degradation and security and privacy concerns [51].Therefore, we assume that operator may offer appealing incentives to encourage users to participate in V2G. In addition, we would like to ensure that each EV participating in V2G will depart with the desired *SoC*. Furthermore, more security measures can be deployed to enhance the security in V2G information and power exchange [40].

One way to leverage V2G is to control the total power load (conventional base load, preconditioning load, minus V2G). Therefore, we design and solve an optimized schedule for EVs which participate in V2G. We consider a slotted time horizon and the objective is to minimize the load on each bus for every time slot by discharging energy from EVs. Each EV which would be discharged to compensate the demand of preconditioning should be charged on subsequent time slots to regain a declared level of SoC inside its predefined deadline.

System model and formulation

We devise a Mixed Integer Linear Problem (MILP) to optimize V2G schedule within the desired preconditioning period. We base our model on a scheduling stretch T which is by itself slotted into smaller time slots n. During T, EVs which are connected to the grid are categorized into two sets I and J. An EV $j \in J$ is going to initiate a pre-conditioning process during T, while EV $i \in I$ is willing to participate in V2G during T within its availability window $[\delta_i, \Delta_i]$. δ_i represents the time slot from where EV i is available for discharging having its full SoC (SoC_i^f), and Δ_i is EV i departure time slot. Once Δ_i is reached EV i must have its desired SoC (SoC_i^d). Any EV of those two sets are considered to be attached with the grid through a bus $b \in B = [1,k]$ where k is the number of buses in the system.

We intend to reduce the total load on each bus for all time slots. Therefore, we define γ_b^n to be the available load bound at bus b during time-slot n. To reduce our multi objective problem we introduce γ_{max} as the maximum available load bound over all the buses and time slots. We seek to lower the maximum load γ_{max} while making sure the total bus load $P_b(n)$ does not exceed its corresponding bus bound γ_b^n. Our mathematical formulation is as follows:

We define the following input parameters:

$$a_j^n = \begin{cases} 1 & \text{if EV } j \text{ is preconditioning during time slot } n \\ 0 & \text{otherwise} \end{cases} \tag{3.6}$$

$$\xi_j^b = \begin{cases} 1 & \text{if EV } j \text{ is connected to bus } b \\ 0 & \text{otherwise} \end{cases} \tag{3.7}$$

$$\rho_i^b = \begin{cases} 1 & \text{if EV} i \text{ is connected to bus } b \\ 0 & \text{otherwise} \end{cases} \tag{3.8}$$

We characterize two decision variables, x_i^n to decide if EV i is being charged during time slot n (as Eq. 3.9), while y_i^n to decide if EV i is being discharged during time slot n (as Eq. 3.10).

$$x_i^n = \begin{cases} 1 & \text{if EV } i \text{ is charging during time slot } n \\ 0 & \text{otherwise} \end{cases} \tag{3.9}$$

$$y_i^n = \begin{cases} 1 & \text{if EV } i \text{ is discharging during time slot } n \\ 0 & \text{otherwise} \end{cases} \tag{3.10}$$

To make sure that EV i is being only charged or discharged during time slot n, we define the following constraint.

$$(x_i^n + y_i^n) \leq 1 \, \forall n; i \in I \tag{3.11}$$

To calculate the bus total load at time period n:

$$P_b(n) = L_b(n) + C_n(n) - D_b(n); \forall b \in B \, ; \forall n; \tag{3.12}$$

$$L_b(n) = \left(\sum_j \left(a_j^n * p * \xi_j^b \right) \right) + H_b(n); \forall b \in B \, \forall n; \tag{3.13}$$

$$C_b(n) = \sum_i \left(x_i^n * \zeta * \rho_i^b \right); \forall b \in B \, \forall n; \tag{3.14}$$

$$D_b(n) = \sum_i \left(y_i^n * d * \rho_i^b \right); \forall b \in B \, \forall n; \tag{3.15}$$

Eq. (3.13) is the amount of power presented on bus b from conventional household power load in addition to preconditioning load during slot n.

Eq.(3.14) is the amount of power drawn from the grid to charge EV i during time slot n on bus b.

Eq. (3.15) is the amount of power fed to the grid from discharging EV i during time slot n on bus b. To ensure that the total bus load L_b does not exceed the bound γ_b^n for all time slots in period T, we demonstrate Eq. (3.16) as:

$$P_b(n) \leq \gamma_n^b; \forall i \in I; \forall b \in B; \forall n; \tag{3.16}$$

Our objective will be to minimize γ_{max}.

$$min\ \gamma_{max} \tag{3.17}$$

$$\gamma_n^b \leq \gamma_{max}; \forall i \in I; \forall b \in B; \forall n; \tag{3.18}$$

Eq. (3.18) ensure that the individual bus bound γ_n^b does not exceed γ_{max}. Once EV i's deadline is reached, its SoC should be equal or greater that the desired SoC according to Eq. (3.19).

$$SoC_i^f + \left(\sum_n x_i^n * c\right) - \left(\sum_n y_i^n * d\right) \geq SoC_i^d; \quad \forall i \in I; \forall n \in [\delta_i, \Delta_i] \tag{3.19}$$

In addition, EV i's schedule should not exceed its deadline.

$$(n - \delta_i)(n - \Delta_i)x_i^n \leq 0; \forall i \in I; \forall n \tag{3.20}$$

$$(n - \delta_i)(n - \Delta_i)y_i^n \leq 0; \forall i \in I; \forall n \tag{3.21}$$

Eq. (3.20) and Eq. (3.21) ensure that neither charging nor discharging will occur outside the availability window of EV i.

3.4.3 Hybrid Solution

Under a lofty power load demand, network reconfiguration might be unsuccessful in alleviating the impact of this high load on the network voltage level [21]. Consequently, some might deploy other methods, such as distributed generations, to enhance the network's voltage level [21]. In addition, after applying V2G, the load supplied by those EVs is considered as negative demand to reduce

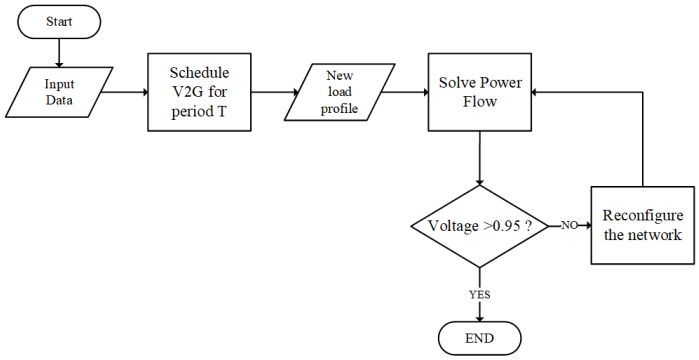

Figure 3.10: The flow chart of the hybrid solution

the bus load. However, the randomness attached to EVs positioning and availability renders V2G somewhat less beneficial by itself. We hence propose a hybrid methodology to use the capabilities of network reconfiguration alongside V2G. In this method, we leverage the load supplied by V2G into the network to reduce the bus load and aid network reconfiguration in compensating the voltage drop in the system. This hybrid solution works in two steps, where in step one we generate new load profile with V2G scheduling, where V2G reduces the load profile of each bus. Afterwards, in the second step, we reconfigure the network at the beginning of each hour of the scheduling period. We will illustrate the operation; we assume we have a number X of EVs willing to participate in V2G, where X is uniformly distributed along all the system buses. We run our scheduler to obtain the optimal V2G process timetable during period T; then we calculate the newly load profiles imposed on each system bus. Subsequently, we apply network reconfiguration (if required) at the beginning of each time slot of period T, where the duration of this time slot is assumed to be one hour. The described method is presented as a flowchart in Fig. 3.10.

3.5 Simulations and Results

We conduct our simulations based on the IEEE-33 bus radial distribution system, where we have the set of vehicles J to have 1623 EVs participating in preconditioning, and set I to have 1650 EVs willing to participate in V2G. For both those sets we only consider level 2 chargers with a charging and discharging rate of 7.2 kW. Each EV in I has a deadline following a truncated normal distribution with a minimum of 10 AM and maximum 12 AM. In addition, each EV in set I has a desired SoC

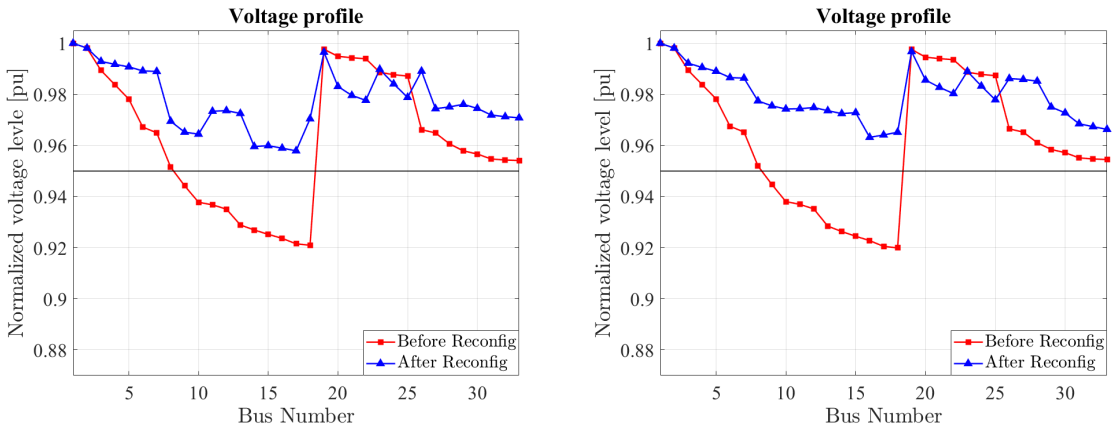

(a) 8AM. (b) 9AM.

Figure 3.11: System voltage profile before and after reconfiguration for $\alpha = \sigma = 50\%$.

to be acquired with a truncated normal distribution with maximum of 90% and minimum 80%.

3.5.1 Network Reconfiguration

To assess the competency of network reconfiguration in improving the performance of the distribution network within operational range, we apply network reconfiguration decided by a Binary Particle Swarm Optimization (BPSO) algorithm [37]. Using this method, we desire to find the optimal network configuration where the losses are minimized and calculate the voltage level of the newly configured buses in the system. In a smart grid we assume reconfiguration can be made in a hourly manner. Therefore, we conduct reconfiguration at the beginning of the time slot.

Fig. 3.11 depicts the voltage profile before and after reconfiguration with 50% EV penetration rate, while level 2 adoption rate is also 50%. Fig. 3.11 shows that reconfiguration improves the voltage drop. In Table 3.1, we represent the optimal configuration for the network and the system quality metrics. We notice that reconfiguration profitably enhances the system metrics where the losses are reduced by an average of 50%, in addition the minimum system voltage is above the operational threshold (0.95 p.u.).

Succeeding, to evaluate the performance of reconfiguration under the stress of a high number of EVs and level 2 charger, we apply reconfiguration for the load profiles generated with $\alpha = \sigma = 80\%$. Fig. 3.12 depicts the system voltage level for each time slot we applied reconfiguration, for both

Table 3.1: Reconfiguration results for $\alpha = \sigma = 50\%$.

Hour	Data	Before	After
8AM	Tie Switches	33 34 35 36 37	7 11 16 28 34
	Power Loss	117.8636 kW	58.1857 kW
	Power Loss Reduction	**********	50.63%
	Minimum Voltage	0.92097 pu	0.96634 pu
9AM	Tie Switches	33 34 35 36 37	7 9 13 15 28
	Power Loss	117.148 kW	57.9038 kW
	Power Loss Reduction	**********	50.57%
	Minimum Voltage	0.91993 pu	0.9632 pu

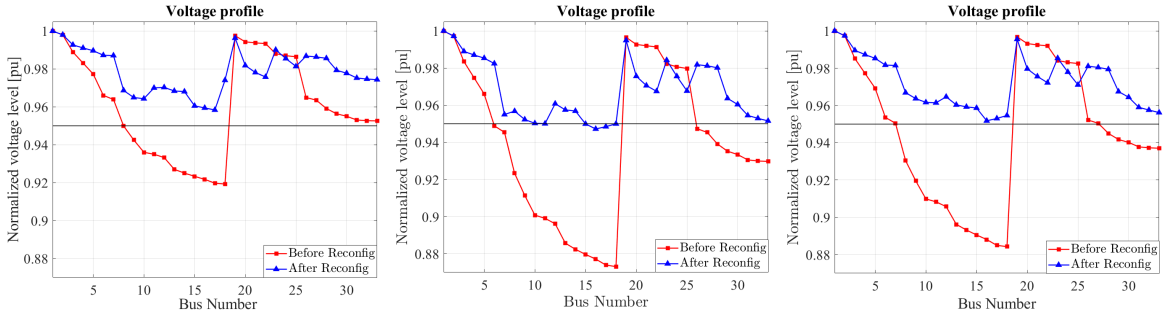

(a) 7AM. (b) 8AM. (c) 9AM.

Figure 3.12: System voltage profile before and after reconfiguration for $\alpha = \sigma = 80\%$.

before and after the process. In this case, we notice that reconfiguration cannot maintain the performance metrics within operational range, as the voltage drop below the acceptable threshold (0.95pu). However, in Table 3.2 the power loss reduction is almost 55%, while the minimum voltage level fails to attain values higher than 0.95 pu. Since, under a high number of EVs and level 2 chargers, reconfiguration fails to assist the network in maintaining an acceptable voltage, we attempt to exploit a number of EVs (i.e., set I) to compensate the large preconditioning demand.

3.5.2 Vehicle-to-Grid Solution

To determine the optimal scheduling for V2G (devised in subsection 3.4.2), we solve the model using a CPLEX solver run on an Intel(R) Core(TM) i7-8750h CPU equipped machine. After obtaining the optimal schedule, we calculate the resultant load profile during the scheduled period.

Table 3.2: Reconfiguration results for $\alpha = \sigma = 80\%$.

Hour	**Data**	**Before**	**After**
7AM	Tie Switches	33 34 35 36 37	7 10 14 17 28
	Power Loss	127.50 kW	65.66 kW
	Power Loss Reduction	**********	48.5%
	Minimum Voltage	0.916 pu	0.958 pu
8AM	Tie Switches	33 34 35 36 37	6 11 14 15 28
	Power Loss	295.65 kW	143.49 kW
	Power Loss Reduction	**********	51.46%
	Minimum Voltage	0.873 pu	0.9472 pu
9AM	Tie Switches	33 34 35 36 37	7 11 15 28 34
	Power Loss	243.55 kW	111.84 kW
	Power Loss Reduction	**********	54.07%
	Minimum Voltage	0.884 pu	0.951 pu

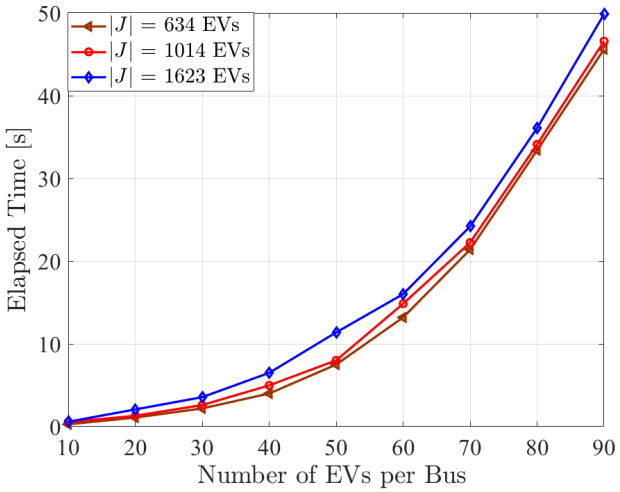

Figure 3.13: Time elapsed for solving the V2G schedule.

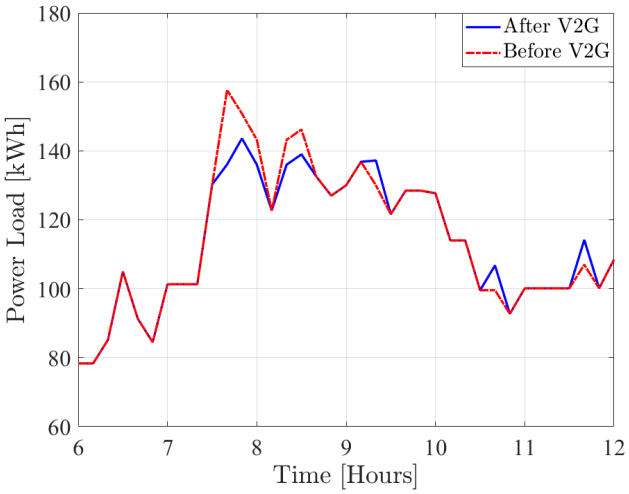

Figure 3.14: Load profile during preconditioning period whit $\alpha = 80\%$.

Afterwards, we feed those profiles to MATPOWER and perform power flow analysis to procure the voltage level on each bus and the system total power losses. Since, reconfiguration fails to provide a satisfactory solution for a higher number of EVs and a higher adoption rate of level 2 chargers, we conduct the scheduling process for the case, where both α and σ are 80%. In our work the purpose of V2G is to reduce the load imposed by preconditioning to assist network reconfiguration in reducing the power losses and enhance the voltage level.

Fig. 3.14 depicts the load profile during preconditioning period for both before and after scheduling of V2G operation, while Fig. 3.15 represents the system voltage level after scheduling EVs for V2G. We notice that V2G reduced the peak load observed during preconditioning period, and enhanced the voltage level and power losses. However, the voltage level did not reach a value above the operational threshold. Therefore, we want to find a way to leverage the reduced load to enhance the network performance. In addition, from Fig. 3.13, it is evident that the computation time of this V2G operation is very small, hence, it is scalable even for a large number of EVs, where for a value of 90 EVs per bus (i.e I=90*33=2970) and high load profile J=1623 we obtained the optimal schedule in 50 seconds.

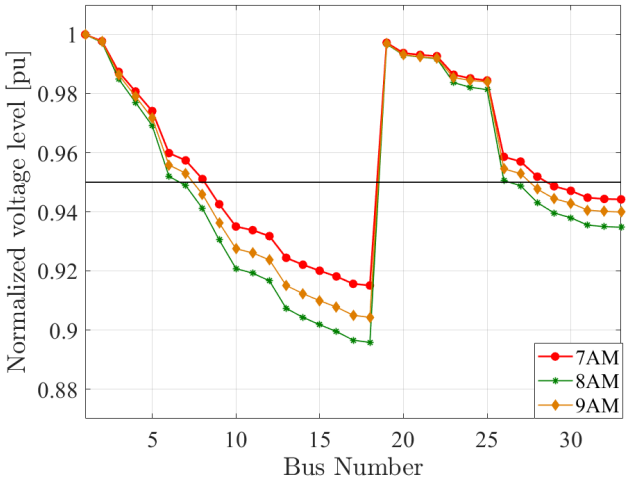

Figure 3.15: System voltage level after V2G for $\alpha = 80\%$.

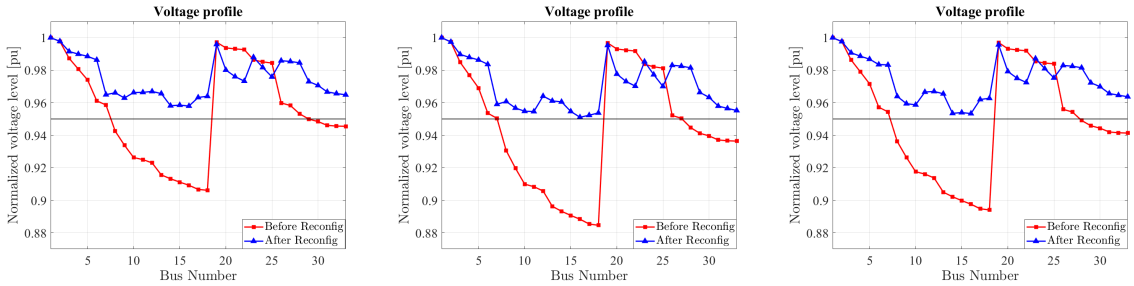

(a) 7AM. (b) 8AM. (c) 9AM.

Figure 3.16: System voltage profile for hybrid solution on static pricing.

3.5.3 Hybrid Methodology

Since, both mitigation techniques (network reconfiguration and V2G solution) failed to stabilize the network performance for a higher number of EVs and level 2 chargers, we propose and apply a hybrid solution to assist the network performance. First, we deploy V2G scheduler for $\alpha = \sigma = 80\%$ and use this schedule to generate the newly reduced load profiles. Afterwards, we reconfigure the network at the beginning of each one hour time slot.

Fig. 3.16 depicts the system voltage level after reconfiguration with V2G generated load profiles. We notice that our hybrid solution successfully enhanced the voltage level to reach a value above operational threshold (0.95 pu). Therefore, the system voltage stability is increased since no bus fail to attain a value higher than 0.95 pu. Table 3.3 represents the optimal network configuration and its performance metrics. We observe that the hybrid solution attained on average 50% power losses

Table 3.3: Reconfiguration results after V2G for $\alpha = \sigma = 80\%$.

Hour	**Data**	**Reconfiguration**	**V2G**	**Hybrid**
7AM	Tie Switches	7 10 14 17 28	33 34 35 36 37	6 9 13 16 28
	Power Loss	65.66 kW	167.85 kW	85.73 kW
	Power Loss Reduction	48.5%	**********	48.92%
	Minimum Voltage	0.958 pu	0.906 pu	0.957 pu
8AM	Tie Switches	6 11 14 15 28	33 34 35 36 37	7 10 13 16 28
	Power Loss	143.49 kW	243.08 kW	120.29 kW
	Power Loss Reduction	51.46%	**********	50.51%
	Minimum Voltage	0.9472 pu	0.884 pu	0.951 pu
9AM	Tie Switches	7 11 15 28 34	33 34 35 36 37	7 10 1316 28
	Power Loss	111.84 kW	206.18 kW	97.38 kW
	Power Loss Reduction	54.07%	**********	52.76%
	Minimum Voltage	0.951 pu	0.89 pu	0.953 pu

reduction and elevated the system's minimum voltage level above 0.95 pu. Hence, we can report that the proposed hybrid solution performs well when there exists a high number of EVs and level 2 chargers with mass EV preconditioning. As attaining a solution from network reconfiguration is almost instantaneous and V2G schedule requires very small time (as shown in Fig. 3.13), the hybrid solution is capable to provide a quick solution to being applicable.

3.6 Conclusion

In this chapter we highlighted the impact of EV preconditioning during winter on the residential radial distribution network. The results showed that preconditioning poses challenges on the distribution network when the number of EVs increases. We observed that alongside elevated winter load demand and EV preconditioning the network could not maintain its voltage level within an operational range, in addition to a high total system power losses. Furthermore, we observed the capability of network reconfiguration and V2G in assisting the network facing those challenges. We realized that reconfiguration can aid the network with the average anticipated EV penetration and

preconditioning, while it failed when this number attains higher rates. Therefore, leveraging this high number of EVs to assist the network, we studied the effects of deploying V2G technology to reduce or shape the high demand profiles, which it reduced the load during preconditioning period but failed to maintain the voltage above 0.95 pu. Accordingly, we proposed a hybrid method to apply V2G scheduling along with network reconfiguration. We observed that reducing the load demand with V2G and reconfiguring the network alleviated the impact of EV preconditioning during winter.

Chapter 4

A Data Driven Performance Analysis Approach for Enhancing the QoS of Public Charging Stations

4.1 Introduction

The newly deployed charging infrastructure is under utilized by users [4]. Indeed, this hesitation in public charging is due to users wanting to avoid long waiting times and outlet uncertainty [5]. This is due to the lack of a practical reservation or a check-in system which keeps track of the waiting times prior to charging as well as the availability of the infrastructure and its utilization. As a consequence, operators resort to approximate the waiting time based on assumptions, such as constant charging rate and constant battery capacity. In addition, their approximations are driven toward specific goals [52] [53] [54] (citing, sizing, profit). Therefore, to estimate the waiting period of an EV at a CS more realistically, this chapter attempts to derive a model for the waiting which is driven by realistic data. Besides the waiting time, we will analyze other CS performance metrics, such as the reneging and blocking probability (rate at which EVs depart from the system prior to charging), which may be used by operators to enhance their deployment of CSs and hence better assist users to minimize their waiting times and improve their experience.

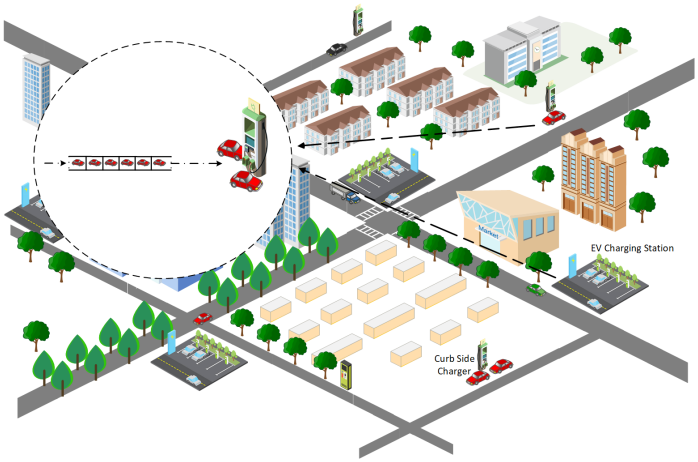

Figure 4.1: System Model.

To enhance the Quality-of-Service (QoS) of public stations and increase its utilisation, we are targeting the following key metrics: average waiting time, reneging probability and blocking probability. This will lead users to have a better understanding of their waiting time and decide on a CS that minimizes that metric. In addition, using the previously mentioned metrics, operators will be able to properly plan the citing and sizing of their CS. Therefore in our work, we will assume a metropolitan area as depicted in figure 4.1, where each CS is modeled as a queuing system with a waiting area (queue) and charging outlets (servers). Figure 4.2 depicts the operational flow which we will follow in our analysis. Initially, we will analyze and extract useful metrics (initial *SoC*, target *SoC*, Battery capacity, charging time) from the real usage data acquired. Since there is no available information about the waiting time, we will study the likelihood of an EV waiting in a CS from the time gap between two consecutive charging session start times. Subsequently, we will devise a charging model guided by real experiments and real CS usage data. After deriving the charging time model, we would like to leverage various variations of the $M/G/k$ queuing system, which compared to the widely used $M/M/k$ in such studies provides a better and more generalized approximation. Finally, we will simulate the operation of the CS. The simulation leverages certain parameters extracted from the real data to verify the waiting time, reneging probability and blocking probability.

The rest of the chapter is organized as follows: in Section 4.2, we present the literature review while in Section 4.3, we analyze the acquired data. Section 4.4 represent our charging model. In Section 4.5, we present our queuing model and in Section 4.6, we present our simulation results.

Finally, in Section 4.7, we conclude the chapter.

4.2 Literature Review

Over the past several years, research efforts have intensified to advance the technology of electric vehicles and its (public and private) charging infrastructure, with the purpose of accelerating the adoption of this technology. Relevant to this work, a thread of research on analytical work has focused on increasing the utilization of the charging infrastructure among EV users by enhancing their performance while maximizing the operators' revenue. The authors in [55] applied a $M/M/c$ queuing model to generate statistical analysis to fit a suitable distribution for the charging demand for Plug-In Hybrid Electric Vehicles (PHEV) at a public charging station and at residences they applied $M/M/c/k/N_{max}$. In their work they utilized a queuing model to fit a distribution for PHEV charging demand. The work of [56] revolve around creating a recommendation system for EV taxis, taking into consideration their time and energy demand. In this work they utilized a general queuing model to assist taxis acquire the longer service time with the shorter waiting time while considering a constant charging rate that result in a unrealistic charging time. In [57] they resort to a predefined charging time distribution to model a charging station with a general queuing model to assist EV on scheduling their sessions in a dual charging modes stations. They utilize a log-normal distribution to describe the charging time. The authors of [58] utilize a general queuing model to create a contract based scheduling scheme. This lead to a specific approximation of the times needed tailored to fit the contract in use. In [59], the authors resorted to $M/M/c$ queue model in order to forecast EV charging demand at rapid charging stations. Afterwards, they generated a spatial and temporal model for EV charging load at those stations using fluid dynamic traffic model to predict EV arrival process. However, their work lacked a generic service time, where they assumed an exponential distribution for such metric. An approach for load balancing among multiple charging stations is proposed in [53], where the objective is to optimize EV charging times. The authors used an $M/M/c$ queue to model EV behavior at public CSs. In their work, they considered that EVs communicate with the grid to share their charging information to allow optimized operation by the grid operators. In [54], a data driven approach is proposed to analyze EV charging

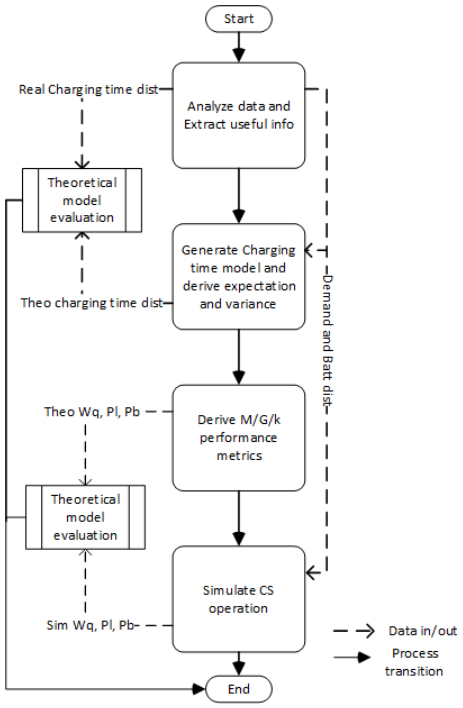

Figure 4.2: System flow chart.

congestion at a CS. Using $M/M/c/k$ queuing techniques, the authors modeled and analyzed the charging congestion at a public CS considering a finite waiting area for the CS. Again, they utilized the exponential distribution for approximating the service time, which lacks the realistic aspect of an EV charging time. In [52] and [60], authors built around citing and sizing CSs. They devised a placement problem around c $(M/M/1)$ queuing models, and they solve the CS sizing problem with $M/M/c$ queuing approach. Again, in this work an exponential service time is used, which is unrealistic. The work of [61] revolved around maximizing the profit from operating a fast CS. Following experimental measurements, they modeled the charging rate as a random variable with a constant battery demand. They modeled the CS as a $M/G/c/k$ queue with a finite waiting area, their goal is to maximize the revenue by deciding the allowed reachable state of charge (SoC) for every admitted EV. Despite using a general charging time distribution, in this work they limit the target SoC and battery size, which is tailored to fit their profit model.

In our work however, we will be devising a real data driven model that can be used for different type of CSs and EVs, in addition to analyze performance metrics with real CS usage data.

4.3 Analytics on Data Set

In order to study and analyze the performance of public charging stations and come up with realistic models which will assist users and operators, we will investigate the CS usage data acquired from our partner (Hydro-Quebec) to get realistic distributions of the operational parameters. The data set at hand is drawn from the charging sessions of 2174 outlets and 68115 members from 2018 till early 2020 over the area of Quebec, and contains multiple key metrics such as charging time, start time and charging demand (*i.e.*, Initial SoC and Final SoC). In addition, the data set contains the utilization metrics of a CS, such as the total charging time for a particular day with the total energy supplied.

Our goal here is to analyze and have a better understanding of the waiting times (*i.e.*, the amount of time an EV will wait before it initiates a charging session). Often, operators are unaware of the times EV users wait at charging poles before accessing the infrastructure and indeed having some information about the statistics of these times can be used by operators to better size and dimension their infrastructure. This can also be fed back to users to make more informed decision about the selection of their charging points. Therefore, using the data set, we would like to estimate the likelihood that an EV has waited before commencing a charging session by studying the inter sessions gap time distribution (*i.e.*, time between start of session k+1 and end of session k). In other words, intuitively, if the inter session gap time is relatively small, we can assume that an EV waited before it started its charging. In figure 4.3 we depict the distribution of the inter session gap time. We observe that the distribution is highly shifted toward the left (small gap values), which indicates a high likelihood that an arriving EV may have waited when another is being charged. However, this assumption cannot give any information about the waiting time.

Another key metric for our analysis is the charging demand. We represent in figure 4.4 the distribution and best fit of the charging demand extracted from the data set. We observe that the charging demand follows a normal distribution, which will be used in our charging model in the coming sections.

Finally, we analyze the inter arrival to the server time distribution. In figure 4.5 we depict this distribution for the extracted parameters from the data. We can observe that this inter arrival time follows

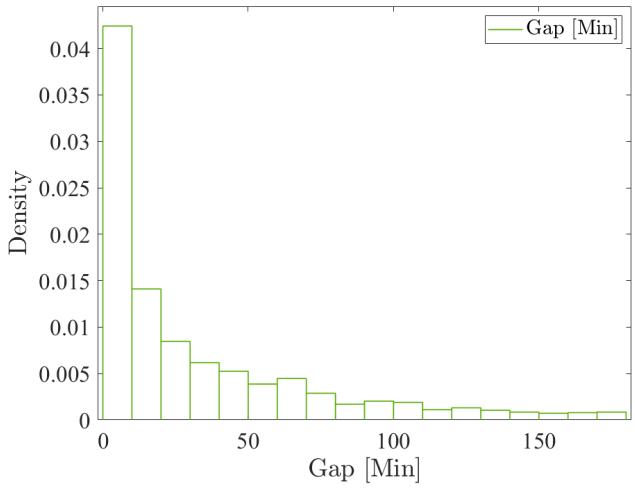

Figure 4.3: PDF of Time Gap between two consecutive sessions.

an exponential distribution.

After completing the previously mentioned data analysis, the necessary initial *SoC*, target *SoC* and battery capacity distribution become available to verify the charging model's performance later on.

4.4 EV Charging Model

In this section, we derive a power model based on the work of [1] where the authors conducted several experiments and charging measurements for a 16kWh battery capacity using ABB's 50kW fast DC charger. In our work, we will differ from the assumption that during a charging session a constant charging rate is maintained and a varying charging rate is adopted which is guided by realistic data extracted from experiments. Each experiment was conducted following different criteria including but not limited to initial SoC, final SoC and battery temperature. Figure 4.6 describes the charger's rate during each charging session. Each curve in this figure represents a different measurement configuration. We adopt the red curve to devise our charging power model since it represents the measurements under normal configuration. We observe from the red curve that the charging power starts as constant and after a certain threshold starts to decrease. We recognize that this decrease can be approximated using a linear model.

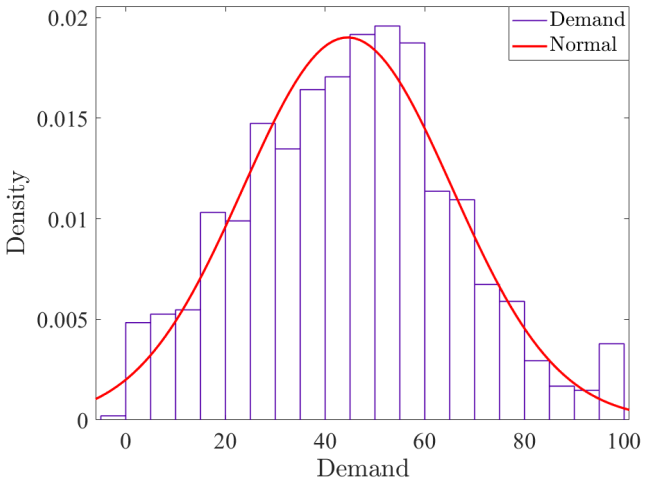

Figure 4.4: PDF of the EV demand.

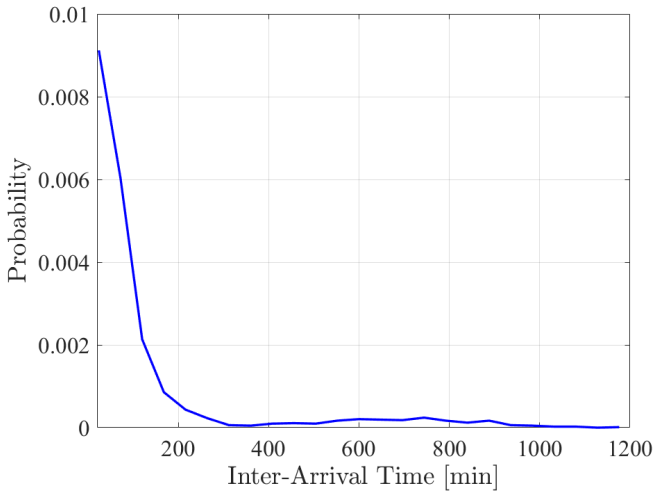

Figure 4.5: Inter-Arrival time distribution from real data.

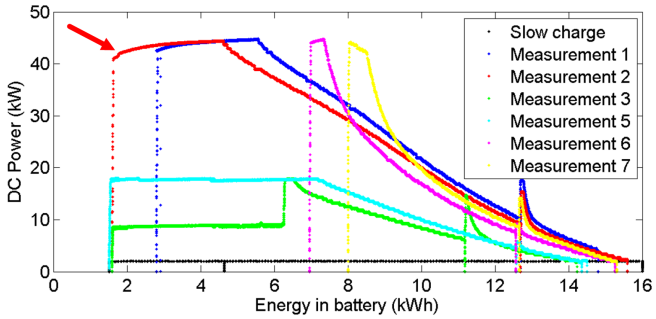

Figure 4.6: Charging rate during battery charging [1]

.

Accordingly, we devise our power model as follows:

$$P(\beta) = \begin{cases} P_{max} & \text{if } \beta < \beta_t \\ -m(\beta) + b & \text{if } \beta \geq \beta_t \end{cases} \tag{4.1}$$

Where P is the charging power (rate) delivered by the charger and β is the energy available inside the battery (battery capacity), β_{max} is the maximum battery capacity, β_t is the threshold battery capacity, m and b are the line component and they are chosen in relation to charger and battery characteristics as follows: $m = \frac{P_{max}}{(1-c)\beta_{max}}$ and $b = \frac{P_{max}}{(1-c)}$ where c is the threshold SoC value (mostly used is 80%). As an example, we depict in figure 4.7 our devised charging model with $\beta_{max} = 20kWh$, $P_{max} = 30kW$, and $\beta_t = 0.8$.

Subsequently, we want to devise a charging time model which will account for the region where the charging rate is decreasing. In addition, the charging time model is a function of the target SoC, in other words, if the user's target SoC is less than the threshold SoC, the user will be served with a constant maximum charging rate. However, if a user decides to go over the threshold SoC, the charging time will consist of two phases, first when the charging rate is constant and second when the rate is decreasing, it is noticeable in [1] that the charging time follows a logarithmic behavior. Thus, our charging time $\mathscr{T}$ is expressed as:

$$\mathscr{T} = \begin{cases} \frac{\beta_r - \beta_i}{P_{max}} & \text{if } \beta_r < \beta_t \\ \delta t_1 + \delta t_2 & \text{if } \beta_r \geq \beta_t \end{cases} \tag{4.2}$$

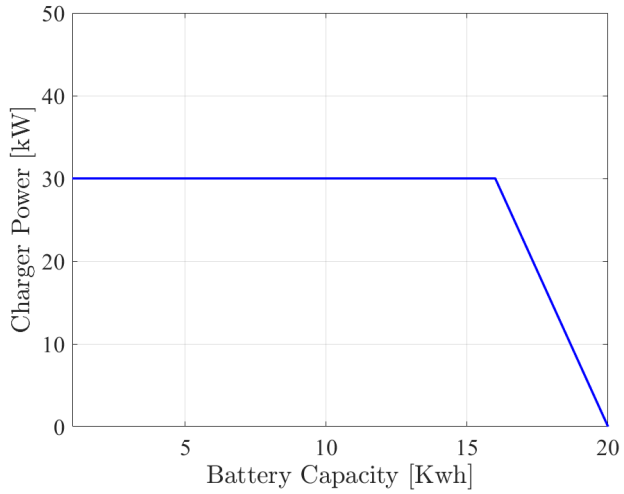

Figure 4.7: Charging model with $\beta_{max} = 20kWh$ and $P_{max} = 30kW$.

With:

$$\delta t_1 = \frac{\beta_t - \beta_i}{P_{max}} \tag{4.3}$$

$$\delta t_2 = \frac{1}{m} \log\left(\frac{b - m\beta_t}{b - m\beta_r}\right) \tag{4.4}$$

In order to verify our model, we compare our formulations with the real charging time data. Following the technical specifications of the DC fast chargers from [6] and [62], we observe that the charging rate differs depending on the type of EV. Some EVs are not compatible with 50kW charging rate and can only operate with 7.2kW. Therefore, in our verification we set P_{max} in the theoretical part to be equal to 30kW. We depict in figures 4.8, 4.9 and 4.10, the theoretical and real charging time distributions for various CSs with different utilization factors. The utilization factor is the amount of time a charger is being used during the amount of time it was plugged. In our study we define high utilization as the highest utilization in the data, the threshold utilization in the data is 60% as medium utilization, and the low utilization as 30%. From figures 4.8, 4.9 and 4.10, we observe high similarity between the distribution of our model and the real data. The similarity indicates that our model can approximate real CS charging time distributions. In addition, we notice that the similarity extends for various utilization factors which in its way describes different EV user behavior and operation modes of CSs.

Now, after deriving the charging time expression, we still require the expectation and variance of

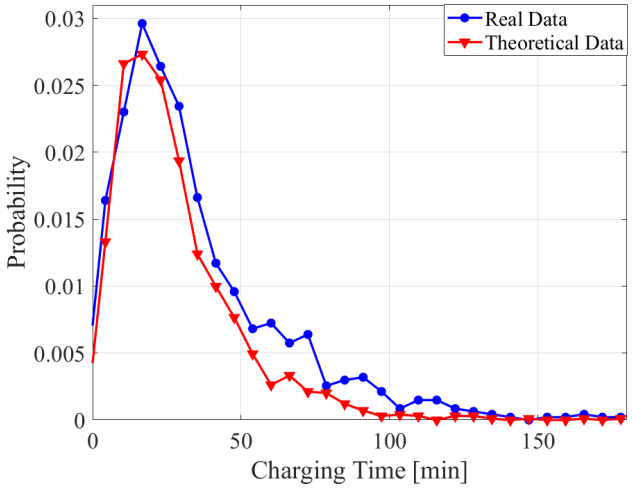

Figure 4.8: Charging Time PDF comparison for high utilization station.

the charging time t in order to utilize this metric as the service time in our upcoming analysis of the $M/G/k$ model. Here, we derive these parameters (expectation and variance) to assist operators which do not have real data to visualize the expected charging time in order to better deploy their charging infrastructure. The derivation of these parameters allows us to finally derive the operational performance metrics such as average waiting time, reneging and blocking probabilities from the queuing model that shall be explained in the coming section.

4.5 Queuing Analysis of a CS

In this section we will derive the expectation and variance of the charging time at a CS. Afterwards, we will leverage a variation of the $M/G/k$ queuing system to analyse the average waiting time, reneging probability and blocking probability.

4.5.1 Derivation of parameters

Initially, we should derive an expression for the expectation ($E[t]$) and variance ($V[t]$) of the charging time model.

Let X, Y and Z denote the random variables characterizing the battery capacity, the initial SoC and the requested SoC, respectively. Hence, we get: $m = \frac{b}{X}$, $b = \frac{P_{max}}{(1-c)}$, $\beta_t = c.X$, $\beta_i = Y.X$ and $\beta_r = Z.X$.

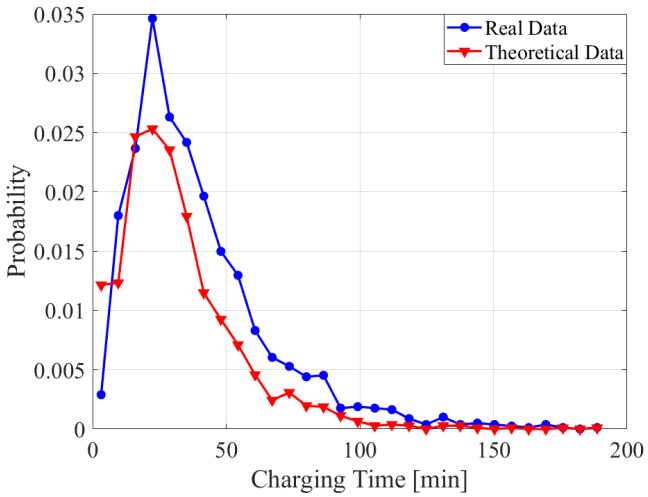

Figure 4.9: Charging Time PDF comparison for average utilization station.

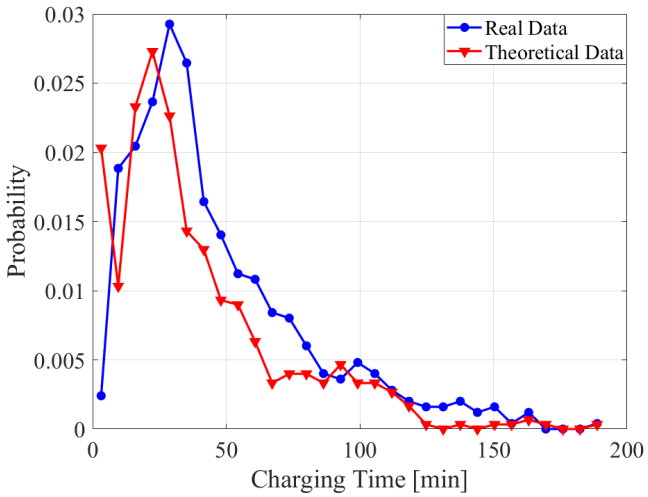

Figure 4.10: Charging Time PDF comparison for low utilization station.

Therefore, we can express t as

$$\mathscr{T} = \begin{cases} \frac{(Z-Y)X}{P_{max}} & \text{if } Z < c \\ \frac{(c-Y)X}{P_{max}} + \frac{(1-c)\log(1-c)}{P_{max}}X - \frac{(1-c)\log(1-Z)}{P_{max}}X & \text{if } Z \geq c \end{cases} \tag{4.5}$$

with:

$$G_1(X,Y,Z) = \frac{(Z-Y)X}{P_{max}}$$

and:

$$G_2(X,Y,Z) \quad = \quad \frac{(c-Y)X}{P_{max}} \quad + \quad \frac{(1-c)\log(1-c)}{P_{max}}X \quad - \quad \frac{(1-c)\log(1-Z)}{P_{max}}X$$

Where the expectation of $E[t]$ can be found by:

$$\begin{aligned} &E[t] = \\ &\int_{X_{min}}^{X_{max}}\int_{Y_{min}}^{Y_{max}}\int_{Z_{min}}^{Z_{max}} f_X(x)f_Y(y)f_Z(z)t(x,y,z)dxdydz \\ &= \int_{X_{min}}^{X_{max}}\int_{Y_{min}}^{Y_{max}}\int_{Z_{min}}^{c} f_X(x)f_Y(y)f_Z(z)G_1(x,y,z)dxdydz \\ &+ \int_{X_{min}}^{X_{max}}\int_{Y_{min}}^{Y_{max}}\int_{c}^{Z_{max}} f_X(x)f_Y(y)f_Z(z)G_2(x,y,z)dxdydz \end{aligned} \tag{4.6}$$

Accordingly, we get:

$$E[\mathscr{T}] = \frac{(E_1[Z]-E[Y])E[X]}{P_{max}} + \frac{(c-E[Y])E[X]}{P_{max}} + \frac{(1-c)\log(1-c)E[X]}{P_{max}} - \frac{(1-c)}{P_{max}}E[X]E_2[\log(1-Z)] \tag{4.7}$$

where $E_1[Z] = \int_{Z_{min}}^{c} zf_Z(z)dz$. Now, using Taylor expectation approximation, the expectation $E[\log(1-Z)]$, can be approximated as

$$E_2[\log(1-Z)] \approx \log(1-E_2[Z]) - \frac{V_2[Z]}{2(1-E_2[Z])^2} \tag{4.8}$$

Where:

$$E_2[Z] = \int_{c}^{Z_{max}} zf_Z(z)dz$$

and

$$V_2[Z] = \int_c^{Z_{max}} (z - E_2[Z])^2 f_Z(z) dz$$

On the other hand, considering the variance of $\mathscr{T}$, it can be expressed as:

$$\begin{aligned} & V[\mathscr{T}] = \\ & \int_{X_{min}}^{X_{max}} \int_{Y_{min}}^{Y_{max}} \int_{Z_{min}}^{Z_{max}} H(x,y,z) f_X(x) f_Y(y) f_Z(z) dx dy dz \\ & = \int_{X_{min}}^{X_{max}} \int_{Y_{min}}^{Y_{max}} \int_{Z_{min}}^{c} H_1(x,y,z) f_X(x) f_Y(y) f_Z(z) dx dy dz \\ & + \int_{X_{min}}^{X_{max}} \int_{Y_{min}}^{Y_{max}} \int_{c}^{Z_{max}} H_2(x,y,z) f_X(x) f_Y(y) f_Z(z) dx dy dz \end{aligned} \tag{4.9}$$

where the functions H, H_1 and H_2 are given, respectively, as

$$\begin{cases} H(x,y,z) = (t(x,y,z) - E[\mathscr{T}])^2 \\ H_1(x,y,z) = (G_1(x,y,z) - E[\mathscr{T}])^2 \\ H_2(x,y,z) = (G_2(x,y,z) - E[\mathscr{T}])^2 \end{cases} \tag{4.10}$$

The above integration (9) will lead to the term $E_2\left[\log(1-Z)^2\right]$. Using Taylor approximation, the expectation $E[\log(1-Z)^2]$ can be approximated as

$$E_2[\log(1-Z)^2] = \log(1 - E_2[Z])^2 - \frac{2(\log(1-E_2[Z]) - 1) V_2[Z]}{(1-E[Z])^2} \tag{4.11}$$

4.5.2 The Average Waiting time

We observe in Figure 4.5 that the inter-server arrival time follows an exponential distribution. In addition, it is clear that the arrival of an EV does not give any information about the next arrival. Therefore, due to its memory-less property the exponential distribution serves as a best approximation for the inter arrival time of the EVs to a CS. Accordingly, in order to study the average waiting time, we model our CS as an $M/G/k$ queuing system.

In the following, we utilize the expressions derived for $E[\mathscr{T}]$ and $V[\mathscr{T}]$ of the charging time $\mathscr{T}$ as the parameter for the service time. We apply different queuing systems to acquire expressions

for the average queuing time (*i.e.* EVs waiting time). Initially, we model our CS as a single server queuing system, with arrival rate λ and service rate μ. We can approximate the waiting time in the queue following the Pollazcek-Khintichine formula (4.12).

$$Lq = \frac{\lambda^2 \sigma_s^2 + \rho^2}{2(1-\rho)} \tag{4.12}$$

such that Lq is the mean number of costumers (EVs) in the system and $\rho = \frac{\lambda}{k(\mu)}$ where k is the number of servers. Using Little's Rule, we can calculate the mean waiting time in the queue as $Wq = \frac{Lq}{\lambda}$.

Afterwards, we model our CS as a multi server queuing system using $M/G/k$ queue with k servers. We apply the Whitt, 1976 and Medhi, 2003 approximation for the average queuing time using (4.13).

$$W_q^{G/G/k} \approx W_q^{M/M/k} \frac{C_a^2 + C_s^2}{2} \tag{4.13}$$

with:

$$W_q^{M/M/k} = \frac{P_0 \left(\frac{\lambda}{\mu}\right)^k \rho}{k!(1-\rho)^2} \tag{4.14a}$$

$$P_0 = \frac{1}{\left[\sum_{i=0}^{k-1} \frac{(k\rho)^i}{i!} + \frac{(k\rho)^k}{k!(1-\rho)}\right]} \tag{4.14b}$$

where $C_a^2 = \frac{\sigma_a^2}{(\frac{1}{\lambda})^2}$ and $C_s^2 = \frac{\sigma_s^2}{(\frac{1}{\mu})^2}$ are the squared coefficient of variation of the arrival time and service time.

4.5.3 Reneging Probability

In this section, we study the reneging effect of EV users on the queuing system. Reneging behavior is defined as the premature departure from a queue without reaching a server. In our case, reneging or loss is defined as an EV departing from a queue after a specific time threshold τ without initiating a charging session. We follow the reneging model in [63] where the authors studied the reneging effect in an $M/G/k$ queuing system and derived a two moment approximation for the loss probability (*i.e.* reneging probability). Let p_l denote the reneging probability which can be

approximated as follows:

$$p_l = (1 - C_s^2) p_l^{det} + C_S^2 p_l^{exp} \tag{4.15}$$

where p_l^{det} and p_l^{exp} are the reneging probability when the service time is deterministic and exponential respectively and these probabilities can be calculated as follows:

$$p_l^{det} = \frac{\frac{r^k}{k!} e^{-\mu\tau(k-r)}}{\sum_{i=0}^{k-1} \frac{k^i}{i!} + \frac{r^k}{k!} \frac{r e^{-\mu\tau(k-r)} - k}{r-k}} \tag{4.16a}$$

$$p_l^{exp} = \frac{(1-r) e^{\mu\tau(r-1)}}{1 - r e^{\mu\tau(r-1)}} \tag{4.16b}$$

with $r = \frac{\lambda}{\mu}$ and τ is the time limit that an EV is willing to wait before deciding to leave the queue without getting service.

4.5.4 Blocking Probability

A useful performance metric for operators of charging infrastructure is the system blocking, which will help is better dimensioning and for EV drivers for better making informed decision. A blocking or deny of service is faced with a limited size parking (waiting) area. An EV will be denied entry to the CS if all the outlets are full and the parking area is full as well. Therefore, in order to model the behavior of a CS with limited parking area, we utilize the $M/G/k/l$ queuing system where k is the number of service channels (outlets) and l is the length of the queue. Since the blocking probability for the latter system does not have a closed form, we follow the approximations for the blocking probability in [64] [65], where p_j is the probability of having j customers in the system, p_j can be approximated as:

$$p_j = \begin{cases} \frac{(k\rho)^j}{j!} p_0' & \text{for } j = 0, ..., k-1 \\ \frac{(k\rho)^k}{k!} \frac{1-\gamma}{1-\rho} \gamma^{j-k} p_0' & \text{for } j = k, ...k+l-1 \\ \frac{(k\rho)^k}{j!} \gamma' p_0' & \text{for } j = k+l \end{cases} \tag{4.17}$$

where:

$$p_0' = \frac{1}{\sum_{i=0}^{k-1} \frac{(k\rho)^i}{i!} + \frac{(k\rho)^k}{k!} \frac{1-\rho\gamma^l}{1-\rho}} \tag{4.18}$$

and:

$$\gamma = \frac{\rho R_G}{1-\rho+\rho R_G}$$

$$\begin{aligned} R_G &= \frac{W_q^{M/G/k}}{W_q^{M/M/k}} \\ &= \frac{(1+C_S^2)}{(2R_D-1)C_S^2+1} \end{aligned}$$

Where a detailed derivation of R_D can be found in [65] and the blocking probability is the probability of having the system full; in other words, the probability of having $k+l$ customers in the system. Finally, we utilize the derived $E[\mathscr{T}]$ and $V[\mathscr{T}]$ in section 4.4 to calculate $\mu = \frac{1}{E[\mathscr{T}]}$ and $\sigma_s^2 = V[\mathscr{T}]$. At this stage, we will have obtained the necessary expressions for the average waiting time, reneging probability and blocking probability. Next, we will verify and analyze the performance of these developed models and expressions through a variety of simulations as presented in the coming section.

4.6 Simulation and Numerical Evaluation

Table 4.1: Simulation parameters.

	Minimum	**Maximum**	**Standard Deviation**	**Average**
Battery Capacity (kWh)	20	100	20	60
Initial SoC ratio	0.1	0.7	0.05	0.4
Target SoC ratio	0.5	0.99	0.05	0.75

Our objective here is to evaluate our derived models. Accordingly, we developed a python based discrete event simulator to verify the performance metrics we derived of the CS queuing model. In our simulation, we extract the input parameters from the data set we have in such a way to imitate

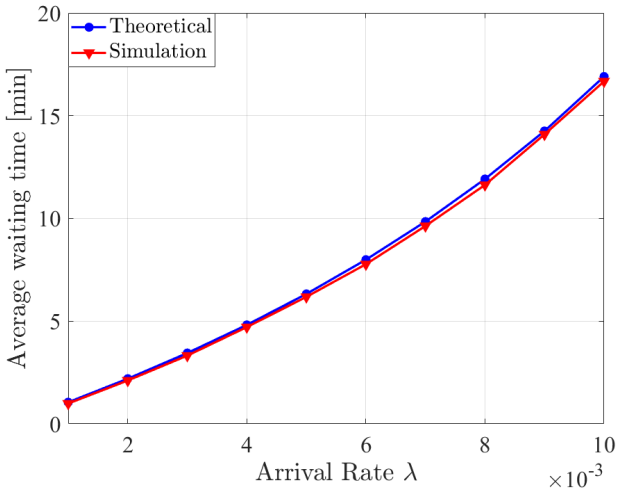

Figure 4.11: Average Waiting time for $M/G/1$ Queuing system.

the performance of the real CSs that the data corresponds to. In our simulations, the demand and battery capacity follows a truncated normal distribution with parameters extracted from the data as shown in table 4.1. In addition, we utilize our derived charging time model to calculate the charging time of each EV. We run our simulation for 100000 EVs with various arrival rates λ keeping $\frac{\lambda}{k\mu} < 1$ to maintain the system's stability. Finally, we set the maximum charging rate $P_{max} = 30kW$ which is the average rate from the EV data and from [6, 62].

We start by analyzing the average waiting time metric; since the data we have does not contain any information about this metric, we rely on the verified simulation to evaluate its theoretical analysis. In figure 4.11, we depict the average time for the $M/G/1$ queuing system from both theoretical studies and preformed simulations. We can observe the increasing nature of this metric with higher arrival rates. Furthermore, we represent in figure 4.12 the same metric for an $M/G/2$ system. The average waiting time shows an increasing trend with increasing arrival rates. The later systems represent a curb-side charger where it can have one or two plugs. We observe from figures 4.11 and 4.12 that the average waiting time decreases when we increase the number of outlets. Therefore, operators can leverage this metric in order to increase their stations' QoS by setting the number of outlets that minimizes the waiting time. Subsequently, we increase the arrival rate range. In figure 4.13, we represent the average waiting time for an $M/G/6$ system that can represent a dedicated public charging station with multiple outlets. The waiting time also increases with higher arrival

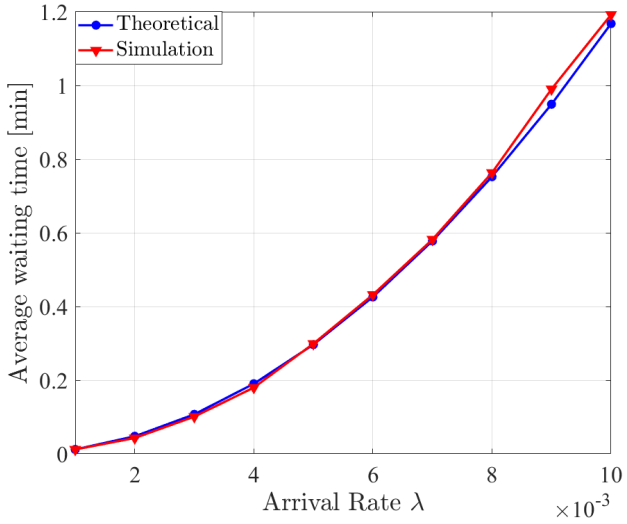

Figure 4.12: Average Waiting time for $M/G/2$ Queuing system.

rates. It should be noted that the maximum arrival rate in a range should not exceed $k\mu$ to keep the system stable. Hence, we can deduce that our model functions as an acceptable approximation for the average waiting time in a public charging station.

Next, we analyze the reneging probability (loss probability) for both $M/G/1$ and $M/G/2$ systems. As mentioned before, reneging probability is the metric to analyze the system when we have impatient customers that decide to prematurely depart before their service starts. We would like to analyze the behavior of these impatient users who depart after a certain threshold τ. Therefore, we calculate the reneging probability for a range of waiting time thresholds τ and various arrival rates λ. In figure 4.14 we depict the reneging probability for an $M/G/1$ system, we notice that the reneging probability decreases when τ increases. Which means that if the users are more patient with waiting the probability of them departing without service decreases. In addition, when the arrival rate increases (*i.e* more customers in the system) the reneging probability increases as well. Afterwards, we analyze the same metric for an $M/G/2$ system. In figure 4.15, we represent the reneging probability of that system. We observe the similar behavior between the reneging probability and τ as well as between probability and λ. However, for more servers we notice that the probability is decreased compared to $M/G/1$. We notice that operators can limit the charging time in their stations in order to increase the number of served EV by decreasing the reneging probability. However, this

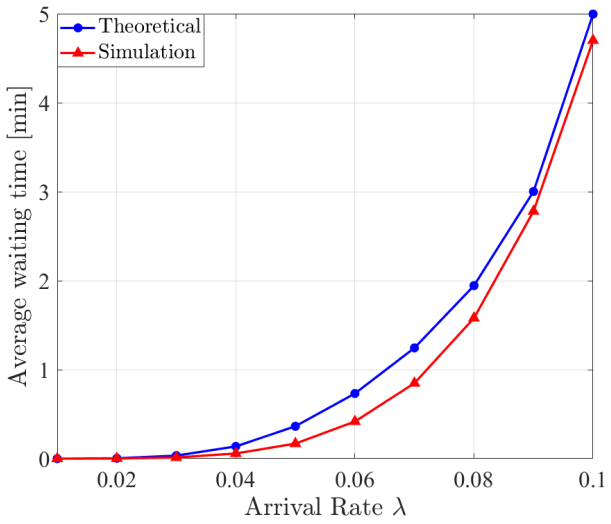

Figure 4.13: Average Waiting time for $M/G/6$ Queuing system.

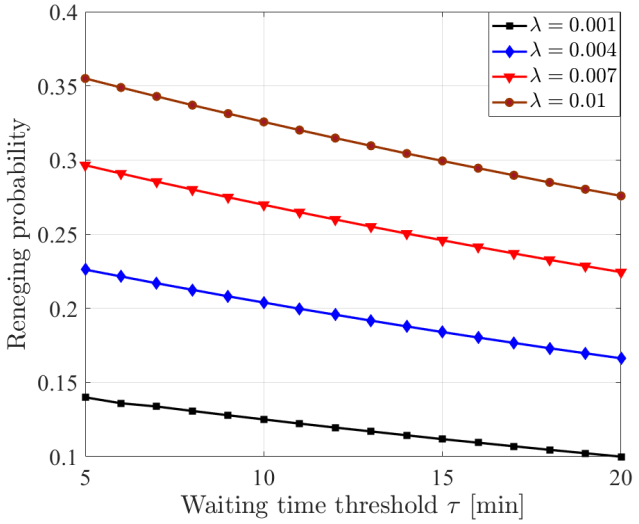

Figure 4.14: Reneging probability for $M/G/1$ Queuing system.

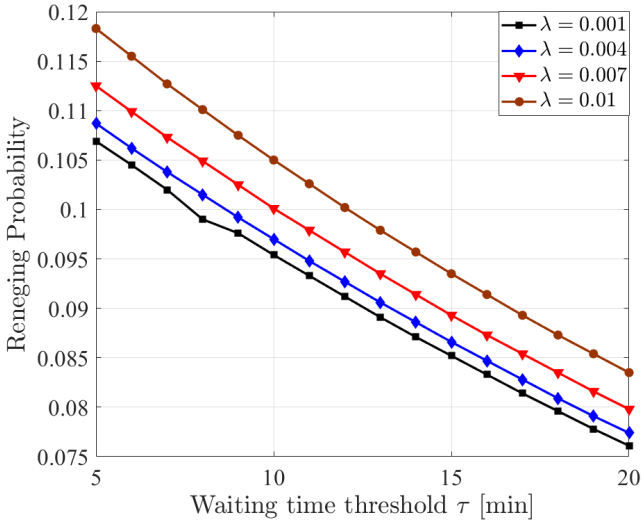

Figure 4.15: Reneging probability for $M/G/2$ Queuing system.

creates a trade-off in the operation of a CS and its scheduling.

Operators might utilize this metric to enhance the deployment process of their charging infrastructure. Indeed, this newly acquired information with a user profiling will give the operators an insight on how to deploy their stations and attain maximum utilization. User profiling consist on surveying the area and have a better understanding about the EV users in that particular area where the CS will be deployed. Information, like size of the family, average waiting time expected among other, will assist operator in determining the size and placement of the deployed CS.

Afterwards, we want to analyze when a CS has a limited parking area. Therefore, we model a CS as an $M/G/1/l$ and $M/G/2/l$ in order to study the blocking probability. Where the blocking probability signifies the probability that a user will arrive to a full CS and will be denied service. In figures 4.16 and 4.17 we depict the blocking probability for the $M/G/1/l$ and $M/G/2/l$ respectively. We notice that with higher arrival rates λ the blocking probability increases. However, we can also notice that with larger parking area the blocking probability tend to decrease. Such type of analysis may help a CS operator to determine the parking capacity based on the arrival rate. By doing so, the operator increases the utilization factor by minimizing the blocking probability.

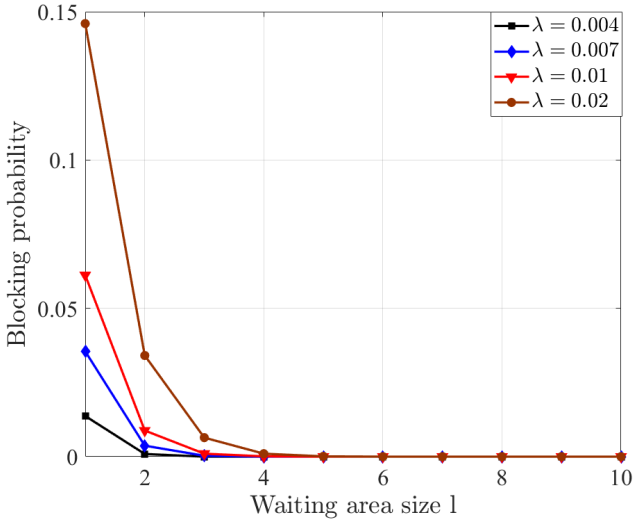

Figure 4.16: Blocking probability for $M/G/1/1+l$ Queuing system.

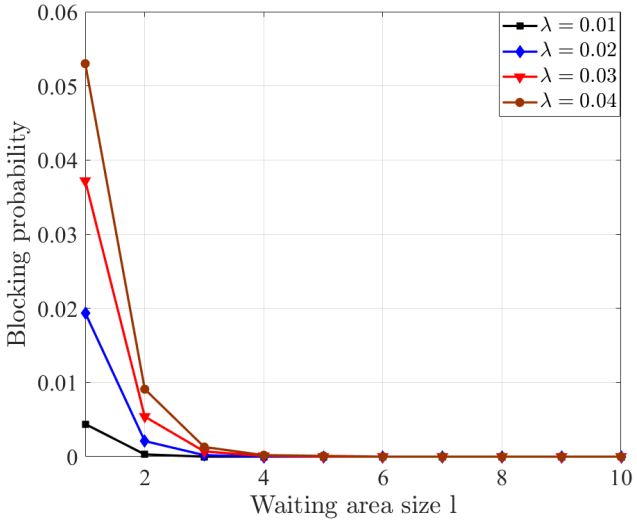

Figure 4.17: Blocking probability for $M/G/2/2+l$ Queuing system.

4.7 Conclusion

In this chapter, we devised a charging time model to study and analyze the performance of an EV public charging station. Afterwards, we utilize our time model into different variations of the $M/G/k$ queuing system to approximate the EV's waiting time, reneging probability and blocking probability at a certain CS. The purpose of our model is to be adaptive to any type or issue that can face a CS in order to find a better solution such as increasing the utilization or enhancing the users' experience. However, since there is a notable and hindering scarcity of real data concerning the waiting time, in future work, we would like for this model to be utilized with intelligent operation models such as smart decisive algorithm to minimize waiting time and increase CS utilization. Additionally, this model can be deployed alongside algorithms to assist operators with placement and sizing of CSs to improve their operation.

Chapter 5

Conclusion and Future Work

In this work various aspects and behavior of mass EV integration were studied. Multiple simulations were conducted to evaluate the impact imposed on the distribution network. From the collected simulations it is noticeable that mass EV charging will create difficult situations to handle for the power network operators. This is categorized by the voltage drop presented in the system when high of EV and level 2 chargers are presented. Additionally, during winter, preconditioning in EV paradigm will bring an elevated load during preconditioning window that mostly occur during off peak times. With strict deadlines preconditioning rendered traditional peak shaping technique, that shift load from peak to off peak obsolete. In order to alleviate the load imposed more adequate mitigation should be utilized or the merger of multiple one to create an potent solution to balance the load and enhance the system voltage level.

Ultimately to increase the number of EVs and work toward a green transportation sector to enhance the environment, it was shown that relying solely on the residential grid will be troublesome since it is noticeable that it might fail when presented with high number of EVs and level 2 chargers. Therefore, the popularity of public dc fast chargers should be increased in order to enhance its utilization and assist users in performing there charging session at those stations. In this work the performance of public CS was studied and an operational model was devised to create a better knowledge on the operation of such CS. Accordingly, with this enhanced information about the operation of public CS user will be able to chose the stations that minimize their overall spent time charging their EVs. In addition, operators will be able to enhance the deployment of their stations to maximize their

utilization and profit.

To enable intelligent and controlled charging ecosystem, it is required to have an interconnected charging infrastructure. This ecosystem is facilitated by two way data sharing. However, this will create more opportunity and attack vectors for adversary users to take advantage and disturb the operation of either the charging infrastructure or the power grid. In [66] a survey over different security aspects of this infrastructure was conducted to analyze the available gaps. In future work, the security aspect of this infrastructure will be studied and effective mitigation will be presented and investigated in securing the charging ecosystem.

Bibliography

[1] D. Andersson and D. Carlsson, "Measurement of abb s prototype fast charging station for electric vehicles," Master's thesis, 2012.

[2] IEA, "Global ev outlook 2019, analysis." [Online]. Available: http://www.iea.org/publications/reports/globalevoutlook2019

[3] P. Chiasson *et al.*, "The shift to electric cars: Are we there yet?" Jul 2018. [Online]. Available: https://montrealgazette.com/news/local-news/the-shift-to-electric-cars-are-we-there-yet

[4] M. of Transportation, "Cars are EVolving," Oct 2013. [Online]. Available: http://www.mto.gov.on.ca/english/vehicles/electric/

[5] Inside EVs Editorial Team, "81% of Electric Vehicle Charging is Done at Home," Apr 2019. [Online]. Available: https://insideevs.com/news/319765/81-of-electric-vehicle-charging-is-done-at-home/

[6] "Electric Vehicle Charging Stations, Technical Installation Guide." [Online]. Available: http://hydroquebec.com/data/electrification-transport/pdf/technical-guide.pdf

[7] "Learn how much it costs to install an electric vehicle charging station." [Online]. Available: https://www.homeadvisor.com/cost/garages/install-an-electric-vehicle-charging-station/#:~:text=Level2chargingpointsuse,findinpublicparkinglots.

[8] Argie and A. Argie, "The true cost of installing an ev charger at home (in canada)," Apr 2019. [Online]. Available: https://csgelectric.ca/the-true-cost-of-installing-an-ev-charger-at-home-in-canada/

[9] J. Lopes *et al.*, "Integration of electric vehicles in the electric power system," *Proceedings of the IEEE*, vol. 99, no. 1, pp. 168–183, 2011.

[10] J. Antoun, M. E. Kabir, B. Moussa, R. Atallah, and C. Assi, "Impact analysis of level 2 ev chargers on residential power distribution grids," in *2020 IEEE 14th International Conference on Compatibility, Power Electronics and Power Engineering (CPE-POWERENG)*, vol. 1, 2020, pp. 523–529.

[11] K. Clement-Nyns *et al.*, "The Impact of Charging Plug-In Hybrid Electric Vehicles on a Residential Distribution Grid," *IEEE Transactions on Power Systems*, vol. 25, no. 1, pp. 371–380, Feb 2010.

[12] A. Dubey and S. Santoso, "Electric vehicle charging on residential distribution systems: Impacts and mitigations," *IEEE Access*, vol. 3, pp. 1871–1893, 2015.

[13] N. Leemput *et al.*, "Impact of electric vehicle on-board single-phase charging strategies on a flemish residential grid," *IEEE Transactions on Smart Grid*, vol. 5, no. 4, pp. 1815–1822, 2014.

[14] Y. Gao *et al.*, "Research on time-of-use price applying to electric vehicles charging," in *IEEE PES Innovative Smart Grid Technologies*. IEEE, 2012, pp. 1–6.

[15] Saeedeh, "Managing Stress of Electric Vehicles on Smart Grids," Dec 2017. [Online]. Available: https://publications.polymtl.ca/2949/

[16] "Electric vehicles sales update q3 2018, canada," Nov 2018. [Online]. Available: https://fleetcarma.com/electric-vehicles-sales-update-q3-2018-canada/.

[17] M. E. Khodayar *et al.*, "Hourly Coordination of Electric Vehicle Operation and Volatile Wind Power Generation in SCUC," *IEEE Trans. Smart Grid*, vol. 3, no. 3, pp. 1271–1279, 2012.

[18] J. Axsen and K. S. Kurani, "The early US market for PHEVs: Anticipating consumer awareness, recharge potential, design priorities and energy impacts," 2008.

[19] J. Cook *et al.*, "Final Evaluation of San Diego Gas & Electric Plug-In Electrical Vehicle TOU," *San Diego Gas & Electric, Tech. Rep*, 2014.

[20] S. Schey *et al.*, "A first look at the impact of electric vehicle charging on the electric grid in the EV project," *World Electric Vehicle Journal*, vol. 5, no. 3, pp. 667–678, 2012.

[21] A. Wazir and N. Arbab, "Analysis and optimization of IEEE 33 bus radial distributed system using optimization algorithm," *JETAE) J. Emerg. Trends Appl. Eng*, vol. 1, no. 2, pp. 2518–4059, 2016.

[22] M. E. Baran and F. F. Wu, "Network reconfiguration in distribution systems for loss reduction and load balancing," *IEEE Power Engineering Review*, vol. 9, no. 4, pp. 101–102, 1989.

[23] L. Hu *et al.*, "Modeling charging behavior of battery electric vehicle drivers: A cumulative prospect theory based approach," *Transportation Research Part C: Emerging Technologies*, vol. 102, pp. 474 – 489, 2019.

[24] L. Hua, J. Wang, and C. Zhou, "Adaptive electric vehicle charging coordination on distribution network," *IEEE Trans. on Smart Grid*, vol. 5, no. 6, pp. 2666–2675, 2014.

[25] R. Taleski and D. Rajicic, "Distribution network reconfiguration for energy loss reduction," *IEEE Trans. on Power Systems*, vol. 12, no. 1, pp. 398–406, 1997.

[26] M. J. E. Alam, K. M. Muttaqi, and D. Sutanto, "A controllable local peak-shaving strategy for effective utilization of pev battery capacity for distribution network support," *IEEE Transactions on Industry Applications*, vol. 51, no. 3, pp. 2030–2037, 2014.

[27] "U.s. energy information administration - eia - independent statistics and analysis." [Online]. Available: https://www.eia.gov/todayinenergy/detail.php?id=29112

[28] T. Moloughney, "Cold weather electric car tips: Maximize your ev for winter," Apr 2019. [Online]. Available: https://insideevs.com/features/342917/cold-weather-electric-car-tips-maximize-your-ev-for-winter/

[29] A. Pesaran, "Ted-aj 03-633 cooling and preheating of batteries in hybrid electric vehicles," 2003.

[30] G. Dao, "Zoe car: why and how to use pre-conditioning?" Jul 2020. [Online]. Available: https://easyelectriclife.groupe.renault.com/en/day-to-day/pre-conditioning-and-your-electric-cars-range/

[31] D. BÃl'langer, P. Gosselin, P. Valois, S. Germain, and B. Abdous, "Use of a remote car starter in relation to smog and climate change perceptions: a population survey in quÃl'bec (canada)," Feb 2009. [Online]. Available: https://www.ncbi.nlm.nih.gov/pmc/articles/PMC2672360/

[32] "National household travel survey." [Online]. Available: https://nhts.ornl.gov/

[33] M. Uddin, M. F. Romlie, M. F. Abdullah, S. A. Halim, T. C. Kwang *et al.*, "A review on peak load shaving strategies," *Renewable and Sustainable Energy Reviews*, vol. 82, pp. 3323–3332, 2018.

[34] J. Antoun, M. E. Kabir, R. Atallah, B. Moussa, M. Ghafouri, and C. Assi, "Impact analysis of EV preconditioning on the residential distribution network," in *2020 IEEE International Conference on Communications, Control, and Computing Technologies for Smart Grids (SmartGridComm) (IEEE SmartGridComm'20)*, Tempe, USA, Nov. 2020.

[35] C. Hunziker, N. Schulz, and H. Wache, "Shaping aggregated load profiles based on optimized local scheduling of home appliances," *Computer Science-Research and Development*, vol. 33, no. 1-2, pp. 61–70, 2018.

[36] N. G. Paterakis, O. ErdinÃğ, A. G. Bakirtzis, and J. P. S. CatalÃčo, "Optimal household appliances scheduling under day-ahead pricing and load-shaping demand response strategies," *IEEE Transactions on Industrial Informatics*, vol. 11, no. 6, pp. 1509–1519, Dec 2015.

[37] O. Badran, S. Mekhilef, H. Mokhlis, and W. Dahalan, "Optimal reconfiguration of distribution system connected with distributed generations: A review of different methodologies," *Renewable and Sustainable Energy Reviews*, vol. 73, pp. 854 – 867, 2017.

[38] C. G. Tse, B. A. Maples, and F. Kreith, "The Use of Plug-In Hybrid Electric Vehicles for Peak Shaving," *Journal of Energy Resources Technology*, vol. 138, no. 1, 09 2015, 011201. [Online]. Available: https://doi.org/10.1115/1.4031209

[39] Yin Yao, Wenzhong Gao, and Yan Li, "Optimization of phev charging schedule for load peak shaving," in *2014 IEEE Conference and Expo Transportation Electrification Asia-Pacific (ITEC Asia-Pacific)*, Aug 2014, pp. 1–6.

[40] Z. Zhou, B. Wang, M. Dong, and K. Ota, "Secure and efficient vehicle-to-grid energy trading in cyber physical systems: Integration of blockchain and edge computing," *IEEE Transactions on Systems, Man, and Cybernetics: Systems*, vol. 50, no. 1, pp. 43–57, 2020.

[41] I. Drovtar, A. Rosin, M. Landsberg, and J. Kilter, "Large scale electric vehicle integration and its impact on the estonian power system," in *2013 IEEE Grenoble Conference*, June 2013, pp. 1–6.

[42] M. E. Baran and F. F. Wu, "Network reconfiguration in distribution systems for loss reduction and load balancing," *IEEE Transactions on Power Delivery*, vol. 4, no. 2, pp. 1401–1407, April 1989.

[43] [Online]. Available: https://data.ukedc.rl.ac.uk/browse/edc/efficiency/residential/LoadProfile

[44] J. Antoun, M. E. Kabir, B. Moussa, R. Atallah, and C. Assi, "Impact analysis of level 2 ev chargers on residential power distribution grids," *IEEE CPE-POWERENG*, 2020 (accepted).

[45] S. Brown, "What is "preconditioning" ?" Oct 2016. [Online]. Available: https://driveev.net/2016/10/24/what-is-pre-conditioning/#.XjhbP2hKjcs

[46] M. Albadi, "Power flow analysis," in *Computational Models in Engineering*, K. Volkov, Ed. Rijeka: IntechOpen, 2020, ch. 5. [Online]. Available: https://doi.org/10.5772/intechopen.83374

[47] R. D. Z. et al., "Matpower: Steady-state operations, planning, and analysis tools for power systems research and education," *IEEE Trans. on Power Systems*, vol. 26, no. 1, pp. 12–19, Feb 2011.

[48] Eep, "Total losses in power distribution and transmission lines: Eep," Dec 2017. [Online]. Available: https://electrical-engineering-portal.com/total-losses-in-power-distribution-and-transmission-lines-1

[49] Jen-Hao Teng, "A direct approach for distribution system load flow solutions," *IEEE Transactions on Power Delivery*, vol. 18, no. 3, pp. 882–887, 2003.

[50] W. Kempton and J. Tomić, "Vehicle-to-grid power implementation: From stabilizing the grenewablid to supporting large-scale re energy," *Journal of power sources*, vol. 144, no. 1, pp. 280–294, 2005.

[51] M. Yilmaz and P. T. Krein, "Review of benefits and challenges of vehicle-to-grid technology," in *2012 IEEE Energy Conversion Congress and Exposition (ECCE)*, 2012, pp. 3082–3089.

[52] M. E. Kabir, C. Assi, H. Alameddine, J. Antoun, and J. Yan, "Demand aware deployment and expansion method for an electric vehicles fast charging network," in *2019 IEEE International Conference on Communications, Control, and Computing Technologies for Smart Grids (SmartGridComm)*, Oct 2019, pp. 1–7.

[53] D. Said, S. Cherkaoui, and L. Khoukhi, "Queuing model for evs charging at public supply stations," in *2013 9th International Wireless Communications and Mobile Computing Conference (IWCMC)*, July 2013, pp. 65–70.

[54] H. Chen, H. Zhang, Z. Hu, Y. Liang, H. Luo, and Y. Wang, "Plug-in electric vehicle charging congestion analysis using taxi travel data in the central area of beijing," *arXiv preprint arXiv:1712.07300*, 2017.

[55] G. Li and X. Zhang, "Modeling of plug-in hybrid electric vehicle charging demand in probabilistic power flow calculations," *IEEE Transactions on Smart Grid*, vol. 3, no. 1, pp. 492–499, March 2012.

[56] Z. Tian, T. Jung, Y. Wang, F. Zhang, L. Tu, C. Xu, C. Tian, and X. Li, "Real-time charging station recommendation system for electric-vehicle taxis," *IEEE Transactions on Intelligent Transportation Systems*, vol. 17, no. 11, pp. 3098–3109, 2016.

[57] Y. Zhang, P. You, and L. Cai, "Optimal charging scheduling by pricing for ev charging station with dual charging modes," *IEEE Transactions on Intelligent Transportation Systems*, vol. 20, no. 9, pp. 3386–3396, 2019.

[58] K. Zhang, Y. Mao, S. Leng, Y. He, S. Maharjan, S. Gjessing, Y. Zhang, and D. H. K. Tsang, "Optimal charging schemes for electric vehicles in smart grid: A contract theoretic approach," *IEEE Transactions on Intelligent Transportation Systems*, vol. 19, no. 9, pp. 3046–3058, 2018.

[59] S. Bae and A. Kwasinski, "Spatial and temporal model of electric vehicle charging demand," *IEEE Transactions on Smart Grid*, vol. 3, no. 1, pp. 394–403, March 2012.

[60] M. E. Kabir, C. Assi, H. Alameddine, J. Antoun, and J. Yan, "Demand-aware provisioning of electric vehicles fast charging infrastructure," *IEEE Transactions on Vehicular Technology*, vol. 69, no. 7, pp. 6952–6963, 2020.

[61] P. Fan, B. Sainbayar, and S. Ren, "Operation analysis of fast charging stations with energy demand control of electric vehicles," *IEEE Transactions on Smart Grid*, vol. 6, no. 4, pp. 1819–1826, July 2015.

[62] C. e. inc., "Ev charging options." [Online]. Available: https://lecircuitelectrique.com/en/charging-options/

[63] S. Bocquet, "Queueing theory with reneging," DEFENCE SCIENCE AND TECHNOLOGY ORGANISATION EDINBURGH (AUSTRALIA) DEFENCE âĂę, Tech. Rep., 2005.

[64] T. Kimura, "A transform-free approximation for the finite capacity m/g/s queue," *Operations Research*, vol. 44, no. 6, pp. 984–988, 1996.

[65] ——, "Approximations for multi-server queues: system interpolations," *Queueing Systems*, vol. 17, no. 3-4, pp. 347–382, 1994.

[66] J. Antoun, M. E. Kabir, B. Moussa, R. Atallah, and C. Assi, "A detailed security assessment of the ev charging ecosystem," *IEEE Network*, pp. 1–8, 2020.